Decline of the North American Avifauna

Authors: Kenneth V. Rosenberg[1,2*], Adriaan M. Dokter[1], Peter J. Blancher[3], John R. Sauer[4], Adam C. Smith[5], Paul A. Smith[3], Jessica C. Stanton[6], Arvind Panjabi[7], Laura Helft[1], Michael Parr[2], Peter P. Marra[8,9]

Affiliations:

[1]Cornell Laboratory of Ornithology, Cornell University, Ithaca, NY 14850, USA.

[2]American Bird Conservancy, Washington, DC 20008, USA.

[3] National Wildlife Research Centre, Environment and Climate Change Canada, Ottawa, ON K1A 0H3, Canada.

[4]Patuxent Wildlife Research Center, United States Geological Survey, Laurel, MD 20708-4017, USA.

[5]Canadian Wildlife Service, Environment and Climate Change Canada, Ottawa, ON K1A 0H3, Canada.

[6]Upper Midwest Environmental Sciences Center, United States Geological Survey, La Crosse, WI, USA.

[7]Bird Conservancy of the Rockies, Fort Collins, CO 80521, USA.

[8]Migratory Bird Center, Smithsonian Conservation Biology Institute, National Zoological Park, PO Box 37012 MRC 5503, Washington, DC 20013-7012, USA.

[9]Current Address: Department of Biology and McCourt School of Public Policy, Georgetown University, 37th and O Streets NW, Washington, DC 20057, USA

*Correspondence to: kvr2@cornell.edu

Abstract: Species extinctions have defined the global biodiversity crisis, but extinction begins with loss in abundance of individuals that can result in compositional and functional changes of ecosystems. Using multiple and independent monitoring networks, we report population losses across much of the North American avifauna over 48 years, including once common species and from most biomes. Integration of range-wide population trajectories and size estimates indicates a net loss approaching 3 billion birds, or 29% of 1970 abundance. A continent-wide weather radar network also reveals a similarly steep decline in biomass passage of migrating birds over a recent 10-year period. This loss of bird abundance signals an urgent need to address threats to avert future avifaunal collapse and associated loss of ecosystem integrity, function and services.

One Sentence Summary: Cumulative loss of nearly three billion birds since 1970, across most North American biomes, signals a pervasive and ongoing avifaunal crisis.

Main Text:

Slowing the loss of biodiversity is one of the defining environmental challenges of the 21st century (*1*–*5*). Habitat loss, climate change, unregulated harvest, and other forms of human-caused mortality (*6*, *7*) have contributed to a thousand-fold increase in global extinctions in the Anthropocene compared to the presumed prehuman background rate, with profound effects on ecosystem functioning and services (*8*). The overwhelming focus on species extinctions, however, has underestimated the extent and consequences of biotic change, by ignoring the loss of abundance within still-common species and in aggregate across large species assemblages (*2*, *9*). Declines in abundance can degrade ecosystem integrity, reducing vital ecological, evolutionary, economic, and social services that organisms provide to their environment (*8*, *10*–*15*). Given the current pace of global environmental change, quantifying change in species abundances is essential to assess ecosystem impacts. Evaluating the magnitude of declines requires effective long-term monitoring of population sizes and trends, data which are rarely available for most taxa.

Birds are excellent indicators of environmental health and ecosystem integrity (*16*, *17*), and our ability to monitor many species over vast spatial scales far exceeds that of any other animal group. We evaluated population change for 529 species of birds in the continental United States and Canada (76% of breeding species), drawing from multiple standardized bird-monitoring datasets, some of which provide close to fifty years of population data. We integrated range-wide estimates of population size and 48-year population trajectories, along with their associated uncertainty, to quantify net change in numbers of birds across the avifauna over recent decades (*18*). We xalso used a network 143 weather radars (NEXRAD) across the contiguous U.S. to estimate long-term changes in nocturnal migratory passage of avian biomass through the airspace in spring from 2007 to 2017. The continuous operation and broad coverage of NEXRAD provide an automated and standardised monitoring tool with unrivaled temporal and spatial extent (*19*). Radar measures cumulative passage across all nocturnally migrating species, many of which breed in areas north of the contiguous U.S. that are poorly monitored by avian surveys. Radar thus expands the area and the proportion of the migratory avifauna that is sampled relative to ground surveys.

Results from long-term surveys, accounting for both increasing and declining species, reveal a net loss in total abundance of 2.9 billion (95% CI = 2.7-3.1 billion) birds across almost all biomes, a reduction of 29% (95% CI = 27-30%) since 1970 (Figure 1; Table 1). Analysis of NEXRAD data indicate a similarly steep decline in nocturnal passage of migratory biomass, a reduction of 13.6 ± 9.1% since 2007 (Figure 2A). Reduction in biomass passage occurred across the eastern U.S. (Figure 2 C,D), where migration is dominated by large numbers of temperate- and boreal-breeding songbirds; we observed no consistent trend in the Central or Pacific flyway regions (Figure 2B,C,D, Table S5). Two completely different and independent monitoring techniques thus signal major population loss across the continental avifauna.

Species exhibiting declines (57%, 303/529) based on long-term survey data span diverse ecological and taxonomic groups. Across breeding biomes, grassland birds showed the largest magnitude of total population loss since 1970—more than 700 million breeding individuals across 31 species— and the largest proportional loss (53%); 74% of grassland species are declining. (Figure 1; Table 1). All forest biomes experienced large avian loss, with a cumulative reduction of more than 1 billion birds. Wetland birds represent the only biome to show an overall

net gain in numbers (13%), led by a 56% increase in waterfowl populations (Figure 3, Table 1). Surprisingly, we also found a large net loss (63%) across 10 introduced species (Figure 3D,E, Table 1).

A total of 419 native migratory species experienced a net loss of 2.5 billion individuals, whereas 100 native resident species showed a small net increase (26 million). Species overwintering in temperate regions experienced the largest net reduction in abundance (1.4 billion), but proportional loss was greatest among species overwintering in coastal regions (42%), southwestern aridlands (42%), and South America (40%) (Table 1; Figure S1). Shorebirds, most of which migrate long distances to winter along coasts throughout the hemisphere, are experiencing consistent, steep population loss (37%).

More than 90% of the total cumulative loss can be attributed to 12 bird families (Figure 3A), including sparrows, warblers, blackbirds, and finches. Of 67 bird families surveyed, 38 showed a net loss in total abundance, whereas 29 showed gains (Figure 3B), indicating recent changes in avifaunal composition (Table S2). While not optimized for species-level analysis, our model indicates 19 widespread and abundant landbirds (including 2 introduced species) each experienced population reductions of >50 million birds (Data S1). Abundant species also contribute strongly to the migratory passage detected by radar (*19*), and radar-derived trends provide a fully independent estimate of widespread declines of migratory birds.

Our study documents a long-developing but overlooked biodiversity crisis in North America—the cumulative loss of nearly 3 billion birds across the avifauna. Population loss is not restricted to rare and threatened species, but includes many widespread and common species that may be disproportionately influential components of food webs and ecosystem function. Furthermore, losses among habitat generalists and even introduced species indicate that declining species are not replaced by species that fare well in human-altered landscapes. Increases among waterfowl and a few other groups (e.g. raptors recovering after the banning of DDT) are insufficient to offset large losses among abundant species (Figure 3). Importantly, our population loss estimates are conservative since we estimated loss only in breeding populations. The total loss and impact on communities and ecosystems could be even higher outside the breeding season if we consider the amplifying effect of "missing" reproductive output from these lost breeders.

Extinction of the Passenger Pigeon (*Ectopistes migratorius*), once likely the most numerous bird on the planet, provides a poignant reminder that even abundant species can go extinct rapidly. Systematic monitoring and attention paid to population declines could have alerted society to its pending extinction (*20*). Today, monitoring data suggest that avian declines will likely continue without targeted conservation action, triggering additional endangered species listings at tremendous financial and social cost. Moreover, because birds provide numerous benefits to ecosystems (e.g., seed dispersal, pollination, pest control) and economies (47 million people spend 9.3 billion U.S. dollars per year through bird-related activities in the U.S. (*21*)), their population reductions and possible extinctions will have severe direct and indirect consequences (*10*, *22*). Population declines can be reversed, as evidenced by the remarkable recovery of waterfowl populations under adaptive harvest management (*23*) and the associated allocation of billions of dollars devoted to wetland protection and restoration, providing a model for proactive conservation in other widespread native habitats such as grasslands.

Steep declines in North American birds parallel patterns of avian declines emerging globally (*14*, *15*, *22*, *24*). In particular, depletion of native grassland bird populations in North America, driven by habitat loss and more toxic pesticide use in both breeding and wintering areas (*25*), mirrors loss of farmland birds throughout Europe and elsewhere (*15*). Even declines among introduced species match similar declines within these same species' native ranges (*26*). Agricultural intensification and urbanization have been similarly linked to declines in insect diversity and biomass (*27*), with cascading impacts on birds and other consumers (*24*, *28*, *29*). Given that birds are one of the best monitored animal groups, birds may also represent the tip of the iceberg, indicating similar or greater losses in other taxonomic groups (*28*, *30*).

Pervasiveness of avian loss across biomes and bird families suggests multiple and interacting threats. Isolating spatio-temporal limiting factors for individual species and populations will require additional study, however, since migratory species with complex life histories are in contact with many threats throughout their annual cycles. A focus on breeding season biology hampers our ability to understand how seasonal interactions drive population change (*31*), although recent continent-wide analyses affirm the importance of events during the non-breeding season (*19*, *32*). Targeted research to identify limiting factors must be coupled with effective policies and societal change that emphasize reducing threats to breeding and non-breeding habitats and minimizing avoidable anthropogenic mortality year-round. Endangered species legislation and international treaties, such as the 1916 Migratory Bird Treaty between Canada and the United States, have prevented extinctions and promoted recovery of once-depleted bird species. History shows that conservation action and legislation works. Our results signal an urgent need to address the ongoing threats of habitat loss, agricultural intensification, coastal disturbance, and direct anthropogenic mortality, all exacerbated by climate change, to avert continued biodiversity loss and potential collapse of the continental avifauna.

References and Notes:

1. M. C. Urban, Accelerating extinction risk from climate change. *Science*. 348, 571–573 (2015).

2. R. Dirzo, H. S. Young, M. Galetti, G. Ceballos, N. J. B. Isaac, B. Collen, Defaunation in the Anthropocene. *Science*. 345, 401–406 (2014).

3. S. L. Pimm, C. N. Jenkins, R. Abell, T. M. Brooks, J. L. Gittleman, L. N. Joppa, P. H. Raven, C. M. Roberts, J. O. Sexton, The biodiversity of species and their rates of extinction, distribution, and protection. *Science*. 344, 1246752–1246752 (2014).

4. A. D. Barnosky, N. Matzke, S. Tomiya, G. O. U. Wogan, B. Swartz, T. B. Quental, C. Marshall, J. L. McGuire, E. L. Lindsey, K. C. Maguire, B. Mersey, E. A. Ferrer, Has the Earth's sixth mass extinction already arrived? *Nature*. 471, 51–57 (2011).

5. W. Steffen, P. J. Crutzen, J. R. McNeill, The Anthropocene: Are Humans Now Overwhelming the Great Forces of Nature. *AMBIO: A Journal of the Human Environment*. 36, 614–621 (2007).

6. S. R. Loss, T. Will, P. P. Marra, Direct Mortality of Birds from Anthropogenic Causes. *Annual Review of Ecology, Evolution, and Systematics*. 46, 99–120 (2015).

7. A. M. Calvert, C. A. Bishop, R. D. Elliot, E. A. Krebs, T. M. Kydd, C. S. Machtans, G. J. Robertson, A Synthesis of Human-related Avian Mortality in Canada. *Avian Conservation and Ecology*. 8 (2013), doi:10.5751/ACE-00581-080211.

8. D. U. Hooper, E. C. Adair, B. J. Cardinale, J. E. K. Byrnes, B. A. Hungate, K. L. Matulich, A. Gonzalez, J. E. Duffy, L. Gamfeldt, M. I. O'Connor, A global synthesis reveals biodiversity loss as a major driver of ecosystem change. *Nature*. 486, 105 (2012).

9. G. Ceballos, P. R. Ehrlich, R. Dirzo, Biological annihilation via the ongoing sixth mass extinction signaled by vertebrate population losses and declines. *Proceedings of the National Academy of Sciences*, 201704949 (2017).

10. C. J. Whelan, Ç. H. Şekercioğlu, D. G. Wenny, Why birds matter: from economic ornithology to ecosystem services. *Journal of Ornithology*. 156, 227–238 (2015).

11. M. Galetti, R. Guevara, M. C. Cortes, R. Fadini, S. Von Matter, A. B. Leite, F. Labecca, T. Ribeiro, C. S. Carvalho, R. G. Collevatti, M. M. Pires, P. R. Guimaraes, P. H. Brancalion, M. C. Ribeiro, P. Jordano, Functional Extinction of Birds Drives Rapid Evolutionary Changes in Seed Size. *Science*. 340, 1086–1090 (2013).

12. G. C. Daily, Ed., *Nature's services: societal dependence on natural ecosystems* (Island Press, Washington, DC, 1997).

13. S. Bauer, B. J. Hoye, Migratory Animals Couple Biodiversity and Ecosystem Functioning Worldwide. *Science*. 344, 1242552–1242552 (2014).

14. K. Gaston, R. Fuller, Commonness, population depletion and conservation biology. *Trends in Ecology & Evolution*. 23, 14–19 (2008).

15. R. Inger, R. Gregory, J. P. Duffy, I. Stott, P. Voříšek, K. J. Gaston, Common European birds are declining rapidly while less abundant species' numbers are rising. *Ecology Letters*. 18, 28–36 (2015).

16. M. L. Morrison, in *Current Ornithology*, R. F. Johnston, Ed. (Springer US, Boston, MA, 1986; http://link.springer.com/10.1007/978-1-4615-6784-4_10), pp. 429–451.

17. J. Burger, M. Gochfeld, Marine Birds as Sentinels of Environmental Pollution. *EcoHealth*. 1 (2004), doi:10.1007/s10393-004-0096-4.

18. Supplemental Materials.

19. A. M. Dokter, A. Farnsworth, D. Fink, V. Ruiz-Gutierrez, W. M. Hochachka, F. A. La Sorte, O. J. Robinson, K. V. Rosenberg, S. Kelling, Seasonal abundance and survival of North America's migratory avifauna determined by weather radar. *Nature Ecology & Evolution*. 2, 1603–1609 (2018).

20. J. C. Stanton, Present-day risk assessment would have predicted the extinction of the passenger pigeon (Ectopistes migratorius). *Biological Conservation*. 180, 11–20 (2014).

21. U.S. Department of the Interior, U.S. Fish and Wildlife Service, and U.S. Department of Commerce, U.S. Census Bureau, "National Survey of Fishing, Hunting, and Wildlife-Associated Recreation." (2016).

22. C. H. Sekercioglu, G. C. Daily, P. R. Ehrlich, Ecosystem consequences of bird declines. *Proceedings of the National Academy of Sciences*. 101, 18042–18047 (2004).

23. J. D. Nichols, M. C. Runge, F. A. Johnson, B. K. Williams, Adaptive harvest management of North American waterfowl populations: a brief history and future prospects. *Journal of Ornithology*. 148, 343–349 (2007).

24. C. A. Hallmann, R. P. B. Foppen, C. A. M. van Turnhout, H. de Kroon, E. Jongejans, Declines in insectivorous birds are associated with high neonicotinoid concentrations. *Nature*. 511, 341–343 (2014).

25. R. L. Stanton, C. A. Morrissey, R. G. Clark, Analysis of trends and agricultural drivers of farmland bird declines in North America: A review. *Agriculture, Ecosystems & Environment*. 254, 244–254 (2018).

26. J. De Laet, J. D. Summers-Smith, The status of the urban house sparrow Passer domesticus in north-western Europe: a review. *Journal of Ornithology*. 148, 275–278 (2007).

27. F. Sánchez-Bayo, K. A. G. Wyckhuys, Worldwide decline of the entomofauna: A review of its drivers. *Biological Conservation*. 232, 8–27 (2019).

28. B. C. Lister, A. Garcia, Climate-driven declines in arthropod abundance restructure a rainforest food web. *Proceedings of the National Academy of Sciences*, 201722477 (2018).

29. D. L. Narango, D. W. Tallamy, P. P. Marra, Nonnative plants reduce population growth of an insectivorous bird. *Proceedings of the National Academy of Sciences*, 201809259 (2018).

30. R. E. A. Almond, M. Grooten, "Living Planet Report - 2018: Aiming Higher" (WWF, Gland, Switzerland, 2018).

31. P. P. Marra, E. B. Cohen, S. R. Loss, J. E. Rutter, C. M. Tonra, A call for full annual cycle research in animal ecology. *Biology Letters*. 11, 20150552 (2015).

32. F. A. La Sorte, D. Fink, P. J. Blancher, A. D. Rodewald, V. Ruiz-Gutierrez, K. V. Rosenberg, W. M. Hochachka, P. H. Verburg, S. Kelling, Global change and the distributional dynamics of migratory bird populations wintering in Central America. *Global Change Biology*. 23, 5284–5296 (2017).

33. J. R. Sauer, W. A. Link, J. E. Fallon, K. L. Pardieck, D. J. Ziolkowski, The North American Breeding Bird Survey 1966–2011: Summary Analysis and Species Accounts. *North American Fauna*. 79, 1–32 (2013).

34. K. V. Rosenberg, P. J. Blancher, J. C. Stanton, A. O. Panjabi, Use of North American Breeding Bird Survey data in avian conservation assessments. *The Condor*. 119, 594–606 (2017).

35. J. C. Stanton, P. J. Blancher, K. V. Rosenberg, A. O. Panjabi, W. E. Thogmartin, Estimating uncertainty of North American landbird population sizes. *Avian Conservation and Ecology*. in press (2019).

36. North American Bird Conservation Initiative, The state of Canada's birds, 2012. *Environment Canada, Ottawa, ON* (2012) (available at http://www.stateofcanadasbirds.org/).

37. North American Bird Conservation Initiative, U.S. Committee, "The State of the Birds, United States of America" (U.S. Department of Interior, Washington, DC, 2009).

38. B. Collen, J. Loh, S. Whitmee, L. McRAE, R. Amin, J. E. Baillie, Monitoring change in vertebrate abundance: the Living Planet Index. *Conservation Biology*. 23, 317–327 (2009).

39. S. N. Wood, *Generalized additive models: an introduction with R* (Chapman and Hall/CRC, 2017).

40. W. A. Link, J. R. Sauer, Bayesian Cross-Validation for Model Evaluation and Selection, with Application to the North American Breeding Survey. *Ecology*, 15-1286.1 (2015).

41. K. Rosenberg, J. Kennedy, R. Dettmers, R. Ford, D. Reynolds, J. Alexander, C. Beardmore, P. Blancher, R. Bogart, G. Butcher, Partners in flight landbird conservation plan: 2016 revision for Canada and continental United States. *Partners in Flight Science Committee* (2016).

42. T. Rich, C. Beardmore, H. Berlanga, P. Blancher, M. Bradstreet, G. Butcher, D. Demarest, E. Dunn, W. Hunter, E. Iñigo-Elias, Partners in Flight North American landbird conservation plan. Ithaca, NY: Cornell Lab of Ornithology (2004).

43. S. Brown, C. Hickey, B. Gill, L. Gorman, C. Gratto-Trevor, S. Haig, B. Harrington, C. Hunter, G. Morrison, G. Page, National shorebird conservation assessment: Shorebird conservation status, conservation units, population estimates, population targets, and species prioritization. *Manomet Center for Conservation Sciences, Manomet, MA* (2000).

44. J. A. Kushlan, M. J. Steinkamp, K. C. Parsons, J. Capp, M. A. Cruz, M. Coulter, I. Davidson, L. Dickson, N. Edelson, R. Elliot, Waterbird conservation for the Americas: the North American waterbird conservation plan, version 1 (2002).

45. North American Bird Conservation Initiative, The State of North America's Birds 2016. *Environment and Climate Change Canada: Ottawa, Ontario* (2016) (available at http://www.stateofthebirds.org/2016/).

46. Partners in Flight, Avian Conservation Assessment Database, version 2017. Available at http://pif.birdconservancy.org/ACAD. Accessed on Nov 5 2018.

47. J. R. Sauer, W. A. Link, Analysis of the North American Breeding Bird Survey Using Hierarchical Models. *The Auk*. 128, 87–98 (2011).

48. J. R. Sauer, D. K. Niven, K. L. Pardieck, D. J. Ziolkowski, W. A. Link, Expanding the North American Breeding Bird Survey Analysis to Include Additional Species and Regions. *Journal of Fish and Wildlife Management*. 8, 154–172 (2017).

49. J. R. Sauer, K. L. Pardieck, D. J. Ziolkowski, A. C. Smith, M.-A. R. Hudson, V. Rodriguez, H. Berlanga, D. K. Niven, W. A. Link, The first 50 years of the North American Breeding Bird Survey. *The Condor*. 119, 576–593 (2017).

50. J. A. Veech, K. L. Pardieck, D. J. Ziolkowski, How well do route survey areas represent landscapes at larger spatial extents? An analysis of land cover composition along Breeding Bird Survey routes. *The Condor*. 119, 607–615 (2017).

51. M. F. Delany, R. A. Kiltie, R. S. Butryn, Land cover along breeding bird survey routes in Florida. *Florida Field Naturalist*. 42, 15–28 (2014).

52. J. A. Veech, M. F. Small, J. T. Baccus, Representativeness of land cover composition along routes of the North American Breeding Bird Survey. *The Auk*. 129, 259–267 (2012).

53. C. M. E. Keller, J. T. Scallan, Potential Roadside Biases Due to Habitat Changes along Breeding Bird Survey Routes. *The Condor*. 101, 50–57 (1999).

54. J. B. C. Harris, D. G. Haskell, Land Cover Sampling Biases Associated with Roadside Bird Surveys. *Avian Conservation and Ecology*. 2 (2007), doi:10.5751/ACE-00201-020212.

55. S. L. Van Wilgenburg, E. M. Beck, B. Obermayer, T. Joyce, B. Weddle, Biased representation of disturbance rates in the roadside sampling frame in boreal forests: implications for monitoring design. *Avian Conservation and Ecology*. 10 (2015), doi:10.5751/ACE-00777-100205.

56. M. G. Betts, D. Mitchell, A. W. Diamond, J. Bêty, Uneven Rates of Landscape Change as a Source of Bias in Roadside Wildlife Surveys. *Journal of Wildlife Management*. 71, 2266 (2007).

57. C. U. Soykan, J. Sauer, J. G. Schuetz, G. S. LeBaron, K. Dale, G. M. Langham, Population trends for North American winter birds based on hierarchical models. *Ecosphere*. 7, e01351 (2016).

58. J. Bart, S. Brown, B. Harrington, R. I. Guy Morrison, Survey trends of North American shorebirds: population declines or shifting distributions? *Journal of Avian Biology*. 38, 73–82 (2007).

59. R. K. Ross, P. A. Smith, B. Campbell, C. A. Friis, R. G. Morrison, Population trends of shorebirds in southern Ontario, 1974-2009. *Waterbirds*, 15–24 (2012).

60. M. E. Seamans, R.D. Rau, "American woodcock population status, 2017" (U.S. Fish and Wildlife Service, Laurel, Maryland, 2017), (available at https://www.fws.gov/birds/surveys-and-data/reports-and-publications/population-status.php).

61. U.S. Fish and Wildlife Service, "Waterfowl population status, 2017" (U.S. Department of the Interior, Washington, D.C. USA, 2017), (available at https://www.fws.gov/birds/surveys-and-data/reports-and-publications.php).

62. Anthony D Fox, James O Leafloor, "A global audit of the status and trends of Arctic and Northern Hemisphere goose populations" (Conservation of Arctic Flora and Fauna International Secretariat, Akureyri, Iceland, 2018).

63. D. J. Groves, "The 2015 North American Trumpeter Swan Survey" (U.S. Fish and Wildlife Service, Juneau Alaska, 2017), (available at https://www.fws.gov/birds/surveys-and-data/reports-and-publications.php).

64. K. V. Rosenberg, P. J. Blancher, in *Bird Conservation Implementation and Integration in the Americas: Proceedings of the Third International Partners in Flight Conference 2002 (C.J. Ralph and T.D. Rich, eds.) PSW-GTR-191* (U.S.D.A. Forest Service, Albany, CA, 2005), vol. 191, pp. 57–67.

65. P. Blancher, K. Rosenberg, A. Panjabi, B. Altman, J. Bart, C. Beardmore, G. Butcher, D. Demarest, R. Dettmers, E. Dunn, Guide to the Partners in Flight Population Estimates Database. Version: North American Landbird Conservation Plan 2004. Partners in Flight Technical Series No 5. *US Geological Survey Patuxent Wildlife Research Center, Laurel, Md* (2007) (available at https://www.partnersinflight.org/resources/pif-tech-series/).

66. P. J. Blancher, K. V. Rosenberg, A. O. Panjabi, B. Altman, A. R. Couturier, W. E. Thogmartin, Handbook to the partners in flight population estimates database, version 2.0. *PIF Technical Series* (2013) (available at http://pif.birdconservancy.org/PopEstimates/).

67. W. E. Thogmartin, F. P. Howe, F. C. James, D. H. Johnson, E. T. Reed, J. R. Sauer, F. R. Thompson, A review of the population estimation approach of the North American Landbird Conservation Plan. *The Auk*. 123, 892 (2006).

68. Sea Duck Joint Venture, "Recommendations for Monitoring Distribution, Abundance, and Trends for North American Sea Ducks" (U.S. Fish and Wildlife Service, Anchorage, Alaska and Canadian Wildlife Service, Sackville, New Brunswick, 2007), (available at http://seaduckjv.org).

69. B. A. Andres, P. A. Smith, R. G. Morrison, C. L. Gratto-Trevor, S. C. Brown, C. A. Friis, Population estimates of North American shorebirds, 2012. *Wader Study Group Bull*. 119, 178–194 (2012).

70. U.S. Shorebird Conservation Partnership, "Shorebird Flyway Population Database (Accessed: 28 Feb 2018)" (2016), (available at https://www.shorebirdplan.org/science/assessment-conservation-status-shorebirds/).

71. P. G. Rodewald (Editor), *The Birds of North America* (Cornell Laboratory of Ornithology, Ithaca, NY, USA, 2018; https://birdsna.org).

72. A. O. Panjabi, P. J. Blancher, W. E. Easton, J. C. Stanton, D. W. Demarest, R. Dettmers, K. V. Rosenberg, Partners in Flight Science Committee, "The Partners in Flight handbook on species assessment Version 2017," *Partners in Flight Technical Series No. 3. Bird Conservancy of the Rockies* (Partners in Flight, 2017).

73. Wetlands International, Waterbird Population Estimates (2018), (available at wpe.wetlands.org).

74. S. Bauer, J. W. Chapman, D. R. Reynolds, J. A. Alves, A. M. Dokter, M. M. H. Menz, N. Sapir, M. Ciach, L. B. Pettersson, J. F. Kelly, H. Leijnse, J. Shamoun-Baranes, From Agricultural Benefits to Aviation Safety: Realizing the Potential of Continent-Wide Radar Networks. *BioScience*. 67, 912–918 (2017).

75. T. D. Crum, R. L. Alberty, The WSR-88D and the WSR-88D Operational Support Facility. *Bulletin of the American Meteorological Society*. 74, 1669–1687 (1993).

76. A. M. Dokter, F. Liechti, H. Stark, L. Delobbe, P. Tabary, I. Holleman, Bird migration flight altitudes studied by a network of operational weather radars. *Journal of The Royal Society Interface*. 8, 30–43 (2011).

77. K. G. Horton, B. M. Van Doren, F. A. La Sorte, E. B. Cohen, H. L. Clipp, J. J. Buler, D. Fink, J. F. Kelly, A. Farnsworth, Holding steady: Little change in intensity or timing of bird migration over the Gulf of Mexico. *Global Change Biology* (2019), doi:10.1111/gcb.14540.

78. S. Ansari, S. Del Greco, E. Kearns, O. Brown, S. Wilkins, M. Ramamurthy, J. Weber, R. May, J. Sundwall, J. Layton, A. Gold, A. Pasch, V. Lakshmanan, Unlocking the Potential of NEXRAD Data through NOAA's Big Data Partnership. *Bulletin of the American Meteorological Society*. 99, 189–204 (2018).

79. A. D. Siggia, R. E. Passarelli, in *Proc. ERAD* (2004), vol. 2, pp. 421–424.

80. J. N. Chrisman, C. A. Ray, in *32nd Conference on Radar Meteorology* (2005).

81. R. L. Ice, R. D. Rhoton, D. S. Saxion, C. A. Ray, N. K. Patel, D. A. Warde, A. D. Free, O. E. Boydstun, D. S. Berkowitz, J. N. Chrisman, J. C. Hubbert, C. Kessinger, M. Dixon, S. Torres, in *23rd International Conference on Interactive Information Processing Systems for Meteorology, Oceanography, and Hydrology* (2007).

82. P. M. Stepanian, K. G. Horton, V. M. Melnikov, D. S. Zrnić, S. A. Gauthreaux, Dual-polarization radar products for biological applications. *Ecosphere*. 7, e01539 (2016).

83. A. M. Dokter, P. Desmet, J. H. Spaaks, S. van Hoey, L. Veen, L. Verlinden, C. Nilsson, G. Haase, H. Leijnse, A. Farnsworth, W. Bouten, J. Shamoun-Baranes, bioRad: biological analysis and visualization of weather radar data. *Ecography* (2018), doi:10.1111/ecog.04028.

84. A. M. Dokter, adokter/vol2bird: vol2bird (Version 0.4.0). Zenodo. (2019), (available at http://doi.org/10.5281/zenodo.3369999).

85. A. M. Dokter, S. Van Hoey, P. Desmet, adokter/bioRad: bioRad (Version 0.4.0). Zenodo. (2019), (available at http://doi.org/10.5281/zenodo.3370005).

86. R. J. Doviak, D. S. Zrnić, *Doppler radar and weather observations* (Dover Publications, Mineola, N.Y, 2nd ed., Dover ed., 2006).

87. T. Chen, C. Guestrin, in *Proceedings of the 22nd ACM SIGKDD International Conference on Knowledge Discovery and Data Mining - KDD '16* (ACM Press, San Francisco, California, USA, 2016; http://dl.acm.org/citation.cfm?doid=2939672.2939785), pp. 785–794.

88. T. Chen, T. He, M. Benesty, V. Khotilovich, Y. Tang, *xgboost: Extreme Gradient Boosting* (2017; https://github.com/dmlc/xgboost).

89. J. Davis, M. Goadrich, (ACM, 2006), pp. 233–240.

90. C. R. Vaughn, Birds and insects as radar targets: A review. *Proceedings of the IEEE*. 73, 205–227 (1985).

91. E. J. Pebesma, Multivariable geostatistics in S: the gstat package. *Computers & Geosciences*. 30, 683–691 (2004).

92. P. M. Stepanian, C. E. Wainwright, Ongoing changes in migration phenology and winter residency at Bracken Bat Cave. *Global Change Biology*. 24, 3266–3275 (2018).

93. A. L. Russell, M. P. Cox, V. A. Brown, G. F. McCracken, Population growth of Mexican free-tailed bats (Tadarida brasiliensis mexicana) predates human agricultural activity. *BMC Evolutionary Biology*. 11 (2011), doi:10.1186/1471-2148-11-88.

94. V. A. Drake, D. R. Reynolds, *Radar entomology: observing insect flight and migration* (Cabi, 2012).

95. S. N. Wood, Fast stable restricted maximum likelihood and marginal likelihood estimation of semiparametric generalized linear models: Estimation of Semiparametric Generalized Linear Models. *Journal of the Royal Statistical Society: Series B (Statistical Methodology)*. 73, 3–36 (2011).

96. Kamil Barton, "MuMIn: Multi-Model Inference" (R package version 1.42.1, 2018), (available at https://CRAN.R-project.org/package=MuMIn).

97. K. P. Burnham, D. R. Anderson, *Model selection and multimodel inference: a practical information-theoretic approach* (Springer, New York, NY, 2. ed., 2010).

98. D. Bates, M. Mächler, B. Bolker, S. Walker, Fitting Linear Mixed-Effects Models Using lme4. *Journal of Statistical Software*. 67 (2015), doi:10.18637/jss.v067.i01.

99. D. W. Winkler, S. M. Billerman, I. J. Lovette, *Bird families of the world: An invitation to the spectacular diversity of birds* (Lynx Edicions, 2015).

100. R. T. Chesser, K. J. Burns, C. Cicero, J. L. Dunn, A. W. Kratter, I. J. Lovette, P. C. Rasmussen, J. V. Remsen, D. F. Stotz, B. M. Winger, K. Winker, Fifty-ninth Supplement to the American Ornithological Society's Check-list of North American Birds. *The Auk*. 135, 798–813 (2018).

Acknowledgments: This paper is a contribution of The Partners in Flight International Science Committee and the American Ornithologist Society Conservation Committee, and the study benefited from many discussions with these groups. Steve Bessinger, John Fitzpatrick, Scott Loss, T. Scott Sillett, Wesley Hochachka, Daniel Fink, Steve Kelling, Viviana Ruiz-Gutierrez, Orin Robinson, Eliot Miller, Amanda Rodewald, and three anonymous reviewers made suggestions to improve the paper. Jillian Ditner and Matt Strimas-Mackey helped with figures and graphics. Tim Meehan provided an analysis of trends from National Audubon's Christmas Bird Count. We thank the hundreds of volunteer citizen-scientists who contributed to long-term bird-monitoring programs in North America and the institutions that manage these programs. Photos in Fig. 3 from Macaulay Library, Cornell Lab of Ornithology.

Funding: NSF LTREB DEB1242584 to PPM; AWS Cloud Credits for Research to AMD; NSF ABI Innovation DBI-1661259.

Author contributions: All authors conceived of the idea for the paper; ACS, PJB, AMD, JRS, PAS, and JCS conducted analyses; KVR, AMD and PPM primarily wrote the paper, although all authors contributed to the final manuscript.

Competing interests: M. P. is President, and a member of the Board of Directors of American Bird Conservancy. All remaining authors declare no competing interests.

Data and materials availability: All data and software are archived and available on Zenodo (DOI 10.5281/zenodo.3218403, 10.5281/zenodo.3369999, 10.5281/zenodo.3370005), and will

be published in future versions of the Avian Conservation Assessment Database (http://pif.birdconservancy.org/ACAD/).

Supplementary Materials:

Materials and Methods

Figures S1-S7

Tables S1-S5

External Databases S1-S2

References (*33-100*)

Figure captions:

Fig. 1. Net population change in North American birds. **(A)** By integrating population size estimates and trajectories for 529 species (*18*), we show a net loss of 2.9 billion breeding birds across the continental avifauna since 1970. Gray shading represents ± 95% credible intervals around total estimated loss. Map shows color-coded breeding biomes based on Bird Conservation Regions and land cover classification (*18*). (**B**) Net loss of abundance occurred across all major breeding biomes except wetlands (see Table 1). (**C**) Proportional net population change relative to 1970, ±95% C.I. (**D**) Proportion of species declining in each biome.

Fig. 2. NEXRAD radar monitoring of nocturnal bird migration across the contiguous U.S. (A) Annual change in biomass passage for the full continental U.S. (black) and **(B)** the Pacific (green), Central (brown), Mississippi (yellow), and Atlantic (blue) flyways (borders indicated in panel C), with percentage of total biomass passage (migration traffic) for each flyway indicated; Declines are significant only for the full U.S. and the Mississippi and Atlantic flyways (Table S3-5). **(C)** Single-site trends in seasonal biomass passage at 143 NEXRAD stations in spring (1 Mar – 1 Jul), estimated for the period 2007-2017. Darker red colors indicate higher declines and loss of biomass passage, while blue colors indicate biomass increase. Circle size indicates trend significance, with closed circles being significant at a 95% confidence level. Only areas outside gray shading have a spatially consistent trend signal separated from background variability. **(D)** 10-year cumulative loss in biomass passage, estimated as the product of a spatially-explicit (generalized additive model) trend, times the surface of average cumulative spring biomass passage.

Fig. 3. Gains and losses across the North American avifauna over the last half century. (A) Bird families were categorized as having a net loss (red) or gain (blue). Total loss of 3.2 billion birds occurred across 38 families; each family with losses greater than 50 million individuals is shown as a proportion of total loss, including two introduced families (gray). Swallows, nightjars, and swifts together show loss within the aerial insectivore guild. (**B**) 29 families show a total gain of 250 million individual birds; the five families with gains greater than 15 million individuals are shown as a proportion of total gain. Four families of raptors are shown as a single group. Note that combining total gain and total loss yields a net loss of 2.9 billion birds across the entire avifauna. (**C**) For each individually represented family in B and C, proportional population change within that family is shown. See Table S2 for statistics on each individual family. (**D**) *Left,* proportion of species with declining trends and, *Right*, percentage population change among introduced and each of four management groups (*18*). A representative species from each group is shown (top to bottom, house sparrow, *Passer domesticus*; sanderling, *Calidris alba*; western meadowlark, *Sturnella neglecta*; green heron, *Butorides virescens*; and snow goose, *Anser caerulescens*).

Species Group	Number of Species	Net Abundance Change (Millions) & 95% CI			Percent Change & 95% CIs			Proportion Species in Decline
		Change	LC95	UC95	Change	LC95	UC95	
Species Summary								
All N. Am. Species	529	-2,911.9	-3,097.5	-2,732.9	-28.8%	-30.2%	-27.3%	57.3%
All Native Species	519	-2,521.0	-2,698.5	-2,347.6	-26.5%	-28.0%	-24.9%	57.4%
Introduced Species	10	-391.6	-442.3	-336.6	-62.9%	-66.5%	-56.4%	50.0%
Native Migratory Species	419	-2,547.7	-2,723.7	-2,374.5	-28.3%	-29.8%	-26.7%	58.2%
Native Resident Species	100	26.3	7.3	46.9	5.3%	1.4%	9.6%	54.0%
Landbirds	357	-2,516.5	-2,692.2	-2,346.0	-27.1%	-28.6%	-25.5%	58.8%
Shorebirds	44	-17.1	-21.8	-12.6	-37.4%	-45.0%	-28.8%	68.2%
Waterbirds	77	-22.5	-37.8	-6.3	-21.5%	-33.1%	-6.2%	51.9%
Waterfowl	41	34.8	24.5	48.3	56.0%	37.9%	79.4%	43.9%
Aerial Insectivores	26	-156.8	-183.8	-127.0	-31.8%	-36.4%	-26.1%	73.1%
Breeding Biome								
Grassland	31	-717.5	-763.9	-673.3	-53.3%	-55.1%	-51.5%	74.2%
Boreal forest	34	-500.7	-627.1	-381.0	-33.1%	-38.9%	-26.9%	50.0%
Forest Generalist	40	-482.2	-552.5	-413.4	-18.1%	-20.4%	-15.8%	40.0%
Habitat Generalist	38	-417.3	-462.1	-371.3	-23.1%	-25.4%	-20.7%	60.5%
Eastern Forest	63	-166.7	-185.8	-147.7	-17.4%	-19.2%	-15.6%	63.5%
Western forest	67	-139.7	-163.8	-116.1	-29.5%	-32.8%	-26.0%	64.2%
Arctic Tundra	51	-79.9	-131.2	-0.7	-23.4%	-37.5%	-0.2%	56.5%
Aridlands	62	-35.6	-49.7	-17.0	-17.0%	-23.0%	-8.1%	56.5%
Coasts	38	-6.1	-18.9	8.5	-15.0%	-39.4%	21.9%	50.0%
Wetlands	95	20.6	8.3	35.3	13.0%	5.1%	23.0%	47.4%
Nonbreeding Biome								
Temperate North America	192	-1,413.0	-1,521.5	-1,292.3	-27.4%	-29.3%	-25.3%	55.2%
South America	41	-537.4	-651.1	-432.6	-40.1%	-45.2%	-34.6%	75.6%
Southwestern Aridlands	50	-238.1	-261.2	-215.6	-41.9%	-44.5%	-39.2%	74.0%
Mexico-Central America	76	-155.3	-187.8	-122.0	-15.5%	-18.3%	-12.6%	52.6%
Widespread Neotdropical	22	-126.0	-171.2	-86.1	-26.8%	-33.4%	-19.3%	45.5%
Widespread	60	-31.6	-63.1	1.6	-3.7%	-7.4%	0.2%	43.3%
Marine	26	-16.3	-29.7	-1.2	-30.8%	-49.1%	-2.5%	61.5%
Coastal	44	-11.0	-14.9	-6.7	-42.0%	-51.8%	-26.7%	68.2%
Caribbean	8	-6.0	1.4	-15.7	12.1%	-2.8%	31.7%	25.0%

Table 1. Net change in abundance across the North American avifauna, 1970-2017. Species are grouped into native and introduced species, management groups (landbirds, shorebirds, waterbirds, waterfowl), major breeding biomes, and nonbreeding biomes (see Data S1 in (*18*) for

assignments and definitions of groups and biomes). Net change in abundance is expressed in millions of breeding individuals, with upper and lower 95% credible intervals (CI) shown. Percentage of species in each group with negative trend trajectories are also noted. Rows colored in red indicate declines and loss; blue rows indicate gains.

Science
AAAS

Supplementary Materials for

Decline of the North American Avifauna

Kenneth V. Rosenberg, Adriaan M. Dokter, Peter J. Blancher, John R. Sauer, Adam C. Smith, Paul A. Smith, Jessica C. Stanton, Arvind Panjabi, Laura Helft, Michael Parr, Peter P. Marra

Correspondence to: kvr2@cornell.edu

This PDF file includes:

Other Supplementary Materials for this manuscript include the following:

Materials and Methods

General approach to estimating long-term net population change

We compiled estimates of long-term population change and current population size for 529 species from a variety of sources (Table S1), as described below. For every species, we selected the most appropriate data sources and assessed the quality of population size and change estimates, based on sampling methodology, range coverage, and precision of the estimates. Our primary source of population change estimates was the North American Breeding Bird Survey (BBS) (*33*), which provides conservation assessment information for hundreds of bird species (*34*). For our current analysis we relied on the full trajectory of population change for each species, which we define as the scaled time-series of annual population indices derived from the underlying trend model. Note that using the full trajectory provides much more information on population change than the simple trend value (% change/yr) usually associated with survey data. We used Partners in Flight's (PIF) recently published population size estimates for North American landbirds (*35*), and we supplemented these with data from several other surveys (Table S1). Values for all U.S./Canada population size estimates, along with their sources, are provided in Data S1.

After compiling population size and trajectory estimates for all species (Data S1), we integrated these into a single hierarchical Bayesian model that estimates the full time-series (1970-2017) of population sizes for each species and for the overall avifauna. Because some species are better monitored than others, the precision of estimates varied greatly among species (Data S1). To reduce the effects of imprecise species-level estimates on our overall estimates of population change, our model included a hierarchical structure that allowed for estimation of composite change based on shrinkage estimators, in which imprecise species results are shrunk toward species-group means based on common ecological biomes in which they breed and overwinter (see below). For summaries, estimates of net population change were computed for four general management categorizations (shorebirds, landbirds, waterbirds, waterfowl), taxonomic familes, and breeding and nonbreeding biomes.

Our hierarchical model of composite change is similar in concept to the bird-group indicator models used to summarize the status of major bird groups at a national level in recent State of the Birds reports in Canada and the United States (*36*, *37*). These indicator models estimate an average population trajectory with respect to a base-year, across species in a group. To this basic group-level model, we added 4 major components: (1) we added a non-parametric smooth to each species estimated population trajectory, accounting for the uncertainty of each annual value, to emphasize the medium- and long-term changes in species populations and reduce the effects of annual fluctuations; (2) we added a second layer to the hierarchical structure to account for influences on each species population trajectory from across the full annual cycle (both nonbreeding and breeding biome); (3) we used the species-level predictions, instead of the group-level trajectories summarized for the State of the Birds reports, as improved estimates of a species population trajectory; and (4) we integrated these improved species trajectories with the species-level population size estimates, to sample the full posterior distribution of population change estimates for each species. The model, an R-script to run it, and all of the orginal data are available on GitHub (https://github.com/AdamCSmithCWS/Rosenberg_et_al).

Data included in the modeling were (1) species (*s*) population indices by year (*y*) and associated variances ($\hat{\imath}_{s,y}, \hat{\sigma}^2_{s,y}$); (2) species population size estimates and associated variances ($\hat{n}_s, \sigma^2_{n_s}$); (3) year(s) in which each species population size was estimated (e.g., most PIF

population estimates represent the species mean population size in the years 2006-2015; ($K_s = 10, k_s = 2006 - 2015$); and (4) information regarding wintering region and breeding biome associations for each species (w = wintering region, b = breeding biome).

Non-parametric smoothing of species' trajectories, centering, and missing data

We used a generalized additive model (GAM) to smooth each species population trajectory ($\hat{\imath}_{s,y}, \hat{\sigma}^2_{s,y}$) before including them in the main model, similar to (*38*). The GAM smooth allowed us to accommodate the wide variation in the underlying population trajectory data and models across the various datasets; for example, some species trajectories have gaps in the time-series when data were not available in a particular year, but were available before and after, and other trajectories are derived from models that allow annual values to fluctuate completely independently, leading to extreme annual fluctuations in relation to other species. Modeling each species trajectory with a flexible smoother retains the most important medium- and long-term patterns in the species' population, and reconciles the level of annual variation among species. We used the R-package mgcv (*39*) to smooth each species trajectory, using a hierarchical Bayesian GAM that accounted for the uncertainty of each annual index in the trajectory to model most species, and for the few species where published estimates of uncertainty were not available (N = 3, Trumpeter Swan, Emperior Goose, and American Woodcock), we used a simpler non-Bayesian GAM function from the same package.

The annual predictions from the GAM smooth ($i_{s,y}, \sigma^2_{s,y}$) for each species and from each data-source were in different units, e.g., BBS estimates are scaled to the number of birds seen on a single route and CBC estimates are scaled to the number observed in an average count-circle. To allow for the hierarchical structure of the model that pools information across groups of species (e.g., grassland birds that winter in Mexico), each species' trajectory was re-scaled to a common base-year (1970) and log-transformed.

$$\hat{\theta}_{s,y} = \ln\left(\frac{i_{s,y}}{i_{s,1970}}\right)$$

Where, $\hat{\theta}_{s,y}$ is the log-transformed standardized annual estimate for year y and species s ($i_{s,y}$) and represents the status of the species in year-y, as a proportion of the original estimate in the base-year, 1970 ($i_{s,1970}$). We calculated the variance of $\hat{\theta}_{s,y}$ as the log transformation of the variance of a ratio of two random variables (Cochran 1977, pg. 183), making the simplifying assuming that the annual estimates are independent in time. We acknowledge that this assumption of independent estimates in time is certaintly invalid for adjacent years, but becomes more plausible as length of the time-series increases

$$\sigma^2_{\hat{\theta}_{s,y}} = \ln\left(1 + \frac{\sigma^2_{i_{s,y}}}{i^2_{s,y}} + \frac{\sigma^2_{i_{s,1970}}}{i^2_{s,1970}}\right)$$

For 8% of species (43), population trajectories spanning 1970-2017 were not available. About half have data-sources that started in the early 1970s and most of the remainder have trajectories starting in the 1990s. In these cases, we assumed that the population did not change during the missing years. Years with missing trajectory information at the beginning of the time-series (e.g., no data before 1993 for some boreal species monitored by the BBS) were given

values equal to the first year with data (i.e. a conservative assumption of no overall change) but we increased the estimated variance ($\sigma^2_{\hat{\theta}_{s,y}}$) by the square of the number of years since non-missing data, so that these imputed data would have little overall effect on the final results. For these species and years, because of the extremely high variance and the hierarchical structure of the model, the modeled population trajectories and the annual number of birds were almost entirely determined by the group-level mean trajectories for the other species sharing the same wintering region and breeding biome.

The primary model: population trajectories accounting for nonbreeding and breeding biome

Each species' estimated status in a given year ($\hat{\theta}_{s,y}$) was treated as a normal random variable with mean $\theta_{s,y}$ and a variance estimated from the species data ($\sigma^2_{\hat{\theta}_{s,y}}$).

$$\hat{\theta}_{s,y} \sim N\left(\theta_{s,y}, \sigma^2_{\hat{\theta}_{s,y}}\right)$$

The the species status parameter $\theta_{s,y}$was assumed to be normally distributed, governed by a hyperparameter ($\mu_{w,b,y}$) with year-specific variance ($\sigma^2_{\mu_y}$),

$$\theta_{s,y} \sim N\left(\mu_{w,b,y}, \sigma^2_{\mu_y}\right)$$

representing mean status for all species with the same combination of wintering range and breeding biome (e.g., all species that winter in South American and breed in the boreal forest). This structure has the effect of shrinking each species population trajectory towards the mean trajectory for species in the same nonbreeding-by-breeding group. The mean trajectories for each group ($\mu_{w,b,y}$) were estimated using an additive sub-model that combined the effects of nonbreeding and breeding biomes. The biome-level components of the additive model were estimated using random-walk time-series for the effects of nonbreeding biomes ($\omega_{w,y}$) and breeding biomes ($\beta_{b,y}$).

$$\mu_{w,b,y} = \omega_{w,y} + \beta_{b,y}$$

$$\omega_{w,y} = N(\omega_{w,y-1}, \sigma^2_{\omega_w})$$
$$\omega_{w,1970} = 0$$

$$\beta_{b,y} = N(\beta_{b,y-1}, \sigma^2_{\beta_y})$$
$$\beta_{b,1970} = 0$$

The random-walk structure has the effect of slightly smoothing large annual fluctuations in the wintering-group annual means, while also allowing for non-linear temporal changes across the 48-year time series.

Integrating the population sizes and population trajectories

Each species' population size estimate was incorporated in the model as the mean ($\hat{n}_s$) and variance ($\sigma^2_{n_s}$) of a normal distribution. Random draws from those distributions (n_s) allowed the model to incorporate the uncertainty around each species' population estimate. We used the

estimated population sizes and the population trajectories during the relevant years represented by each species' population estimate to calculate a scaling factor (ψ_s) that allowed us to re-scale the species estimated population trajectory (θ_{s,y_i}) to an estimated number of birds in each year of the time-series ($\nu_{s,y}$). Each population estimate was related to a specific year or range of years; e.g., all PIF population estimates reflect the species' mean population size between 2006 and 2015 ($K_s = 10, k = 2006 - 2015$). We estimated the scaling factors by averaging the ratio across the relevant span of years, with $K_s = 3$ as a minimum in a few cases where the species' estimated population reportedly related to a single year.

$$\psi_s = \frac{\sum_{y_i}^{y_k} \left(\frac{n_s}{\exp(\theta_{s,y_i})} \right)}{K_s}$$

$$\nu_{s,y} = \psi_s * \theta_{s,y}$$

All precision parameters were given diffuse gamma prior distributions, with scale and shape parameters set to 0.001. Formal measures of model fit are difficult to implement for complex hierarchical models, and are generally not presented for analyses of complex surveys (*40*). We used graphical comparisons between data and predictions (see additional figures available in the data and code repository) to ensure there was no important lack of fit between the model and the data.

Annual number of birds and overall population change

We calculated the overall population change by species (λ_s) using the posterior distribution of the difference between the estimated number of birds in 1970 and the number in 2017. We calculated the estimated number of birds in the North American avifauna for each year (N_y) using the posterior distribution of the annual sums of all species estimates. We calculated the overall net change in the North American avifauna using the posterior distribution of the sum of the species-level change estimates (Λ). Estimates of the annual number of birds (N_y) and overall change (Λ) by family, nonbreeding biome (Figure S1), breeding biome (Figure 1A), and combinations of nonbreeding and breeding biome (Figure S2) were made from the posterior distribution of group-level summaries across all S-species in a group.

$$\lambda_s = \nu_{s,1970} - \nu_{s,2017}$$

$$N_y = \sum_{s_i}^{S} (\nu_{s,y})$$

$$\Lambda = \sum_{s_i}^{S} (\lambda_s)$$

Sources of Population Trajectories for North American Birds

We compiled long term population trajectories for 529 species, based on the best available survey data for each species (Table S1; see Data S1 for species-specific information). We note that this compilation reflects standard data sources used by North American bird conservation and management (*23*, *36*, *41–45*). We are fortunate that standardized, long-term survey data exist for a majority of North American bird species, perhaps the best-monitored group of organisms

globally. We used trajectory estimates based on surveys of breeding populations whenever possible; however not all species are well-monitored during the breeding season, and for 18% of species we relied on surveys from migration periods or winter (Table S1). In all cases, trajectories and population estimates for each species were calculated from data during the same season (i.e., breeding to breeding, winter to winter). We could not find credible surveys for estimation of continent-scale trajectories for oceanic birds, many coastal-nesting seabirds, and other rare, secretive, range-restricted or nocturnal species. However, our synthesis includes 76% of species that breed regularly in the continental U.S. and Canada (*46*), and these species likely account for 95%-99% of total breeding abundance across the North American avifauna (i.e., most species omitted have very small populations in the U.S. and Canada).

For 434 species (82% of 529 species considered) we used trajectories from BBS data, most of which are updated annually and publicly available at https://www.mbr-pwrc.usgs.gov/. For species surveyed by the BBS, a hierarchical model (*47*) was used to estimate annual indices of abundance. In our hierarchical analysis, annual indices are based on regional fits within states and provinces that are weighted by area and local abundance to accommodate differences in population sizes among strata. For a majority of species (415) we used data from the 'core' BBS area from 1970-2017, based on road-based survey routes in the contiguous U.S. and southern Canada. For 19 species with restricted or northern breeding distributions (See Data S1), we used data from an expanded analysis beginning in 1993, including additional BBS routes in Alaska and northern Canada (*48*). The proportion of each species' breeding range covered by the BBS is provided in (*33*), and all metadata and data are available (https://www.pwrc.usgs.gov/bbs/).

Potential limitations or biases in BBS trends (overall rates of change across the trajectories) have been extensively examined and documented (e.g., (*33*, *49*)). In general, there is no evidence to suggest that estimates of population trends from the BBS are systematically biased across large spatial areas or across many species. Published studies that have examined the potential roadside bias in BBS trends have found that the magnitudes of bias in the sampling of habitat-change are generally small, e.g. (*50–53*), that potential biases vary in space (e.g., contrasting biases in the regions used in (*54*), or in (*55*)), and that they vary among species (i.e., if biases exist, some species' trends may be underestimated and others overestimated, e.g., (*55*, *56*)). Overall, BBS routes survey a reasonably representative sample of the overall habitat in the landscape at the broad spatial and temporal scales, for which the BBS was designed (*50*).

National Audubon Society Christmas Bird Counts (*57*) provided trajectory data for 58 species; these are primarily species that breed in northern regions not surveyed by the BBS, but are encountered in CBCs because they spend the non-breeding season primarily within the U.S. and southern Canada. The CBC protocols are less standardized than BBS, but annual winter-season counts in fixed 15-mile diameter circles cover a large portion of the U.S. and Canada, especially in coastal regions. Trajectories from CBC data were estimated using a hierarchical model that controlled for effort (*57*). Annual indices to compute trajectories from the CBC for the 1970-2017 period were provided to us by Tim Meehan (National Audubon).

Trajectories for 20 species of long-distance migrant shorebirds came from an analysis of migration monitoring surveys carried out across Canada and the United States (*58*, *59*). The shorebird migration surveys used here are part of the International Shorebird Survey, coordinated by Manomet, and the Atlantic Canada and Ontario Shorebird Surveys, coordinated by Environment and Climate Change Canada. Volunteers carry out surveys every 10 days in spring and fall, at sites distributed across Canada and the United States but concentrated primarily in the eastern half of the continent. Analyses of shorebird trajectories from fall count data, 1974-2016,

were carried out using hierarchical Bayesian models similar to those used for the BBS (*47*), with an additional General Additive Model (GAM) component to describe variation in birds' abundance during the period of migratory passage. The model assumes that counts follow an overdispersed Poisson distribution, and includes terms for a long-term, log-linear trend, year-effects and site-level abundance. Sites were grouped into biologically relevant regions, and trend terms within each region were estimated as hierarchical random effects distributed around a mean, continental trend. Methods and survey coverage are described in more detail at wildlife-species.canada.ca/bird-status (https://tinyurl.com/yak95ssn). For one shorebird species, American Woodcock, we made use of Singing-ground Survey estimates from the 2017 American Woodcock Status report (*60*).

For nine species of intensely managed waterfowl we relied on trajectory data from the U.S. Fish and Wildlife Service (USFWS) (*61*), and trajectories for nine additional waterfowl species came from other species-specific sources (see Table S1, Data S1). Trajectories for many waterfowl species were computed using population estimates from Spring Breeding Ground Surveys, which use a combination of aerial and ground-based counts in late spring, covering 2.0 million square miles in Alaska, Canada, and the northern U.S. (Table c3 in (*61*)). For a small subset of species, we employed other sources of trajectory information where this resulted in better coverage of North American populations, and/or more current information. For all goose species we relied on estimated trajectories from the same sources of information on population trends reported for North American goose populations by Fox and Leafloor (*62*); these sources represent the most appropriate survey for each species as determined by experts on goose populations. Finally, for Trumpeter Swans we relied on values in the 2015 North American Trumpeter Swan Survey report (*63*).

Sources of Population Size Estimates and Variances

We relied on the best available data sources and published estimates of North American breeding population size and variance for all species with credible data (Table S1; Data S1). The largest source of population estimates for our current analysis (65% of species) was the recently published PIF estimates for 344 landbird species (*35*). The PIF estimates were based on extrapolations from BBS count data from 2006-2015, using previously described methods (*64–67*). Averaged annual BBS counts were converted to a regional (landscape-scale) abundance estimate through the application of detectability adjustment factors for time-of-day, detection distance, and likelihood of both members of a pair being detected on BBS routes, and extrapolation from BBS count area to area of the region. These regional estimates are calculated for each state, province and territory portion of each Bird Conservation Region (BCR), and then summed across regions to derive U.S.-Canada population estimates. Estimates incorporated uncertainty in the estimation components, resulting in confidence bounds around the final estimates (*35*). Population estimates are therefore adjusted for detection, account for variation in relative abundance across the species' range, and are accompanied by a measure of uncertainty. This approach to estimation of total population size has been widely adopted in conservation planning (*35*), and is considered to be conservative, likely underestimating true population size due to sampling concerns associated with BBS data (*67*).

The PIF methods for estimating population size have historically been applied only to landbirds (*41*, *42*). For this analysis, we determined that the BBS also provides adequate survey coverage for 46 waterbirds, and 6 waterfowl that otherwise were lacking useful population estimates (see Data S1 for sources by species), and we applied the PIF approach for calculating

population size estimates to data for these species. Adjustment factors used in the estimation of U.S.-Canada population sizes for the current analysis, based on BBS relative abundances, are provided in Table S2. More details on the use of adjustment factors and their ranges of uncertainty for landbirds can be found in (*35*).

Estimates of population size for many shorebirds and waterfowl came from published sources that rely on other surveys. Estimates for 12 waterfowl species were from the 2017 USFWS Waterfowl Status Report (*61*) (7 species from traditional area surveys, 2 from eastern survey area, 2 summed from traditional and eastern surveys, and 1 from western survey area) – for these species, we used an average of published estimates across the last 5 years (2013-2017) to smooth out annual variance in population sizes. Estimates for 14 additional waterfowl species were based on a 2007 Seaduck Joint Venture Report (*68*). All 45 shorebird species estimates were North American population estimates (*69*) from the Shorebird Flyway Population Database (*70*).

Other estimates of population size came from species-specific sources (Table S1; Data S1): We used published estimates from Birds of North America (BNA) accounts (*71*) for 33 species; a Conservation of Arctic Flora and Fauna (CAFF) 2018 report provided current estimates for 7 goose species (*62*); estimates for 17 landbird species without useful BBS-based estimates were taken from the Avian Conservation Assessment Database ACAD (*46*, *72*), which itself relied on a variety of sources; the 2015 North American Trumpeter Swan Survey (*63*) was used for Trumpeter Swan, and the Waterbird Population Estimates database (WPE5) provided estimates for Arctic Tern (*73*).

Most sources of population estimates also provided estimates of variance in population size, which we incorporated into our analysis. For those that did not, we estimated a range of variance based on a description of methods used for population estimation. For example, we applied a range 10% below and above the mean for species if estimates were based on well-designed surveys with good population coverage, versus 75% below and above the mean for species with ballpark estimates and/or low coverage of relevant populations, with an intermediate range of variance if limitations were between those two.

Note that our goal was to compile and use the most current estimates of breeding population size for each species; i.e., the number of breeding adult individuals in the population. We did not attempt to estimate the annual increase in population size due to the influences of reproductive output, as this will likely vary greatly across species and years and be subject to density-dependent effects. Total population size varies throughout the annual cycle, but post-breeding total population could increase as much as four to five times the size of the pre-breeding population size depending on recruitment success of young of the year. Estimating this annual variation for individual species is currently impossible, but it is important to point out that the cumulative impact of population loss on ecosystems throughout the year could be quite significant. Our estimates of population change are therefore conservative.

Assigning species to management and biome categories

For the purpose of summarizing changes in abundance across the North American avifauna, we recognize four broad species categories used for management and conservation planning: *Landbirds* are defined by Partners in Flight (*41*, *42*) as all birds occupying terrestrial habitats and a few species from primarily terrestrial bird families that use wetland habitats (e.g., Marsh Wren, *Cistothorus palustris*). The ACAD lists (448) native landbirds breeding in the U.S. and Canada; in this paper we include 366 landbird species with adequate population size and trajectory data, including 9 introduced species. *Shorebirds* include all sandpipers, plovers, stilts, avocets, and oystercatchers that are considered under the U.S. Shorebird Conservation Partnership

(*43*); we had adequate data for 45 shorebird species for the current analysis. *Waterfowl* include all ducks, geese, and swans, which are managed separately under the North American Waterfowl Management Plan; most species have populations that are adaptively managed for sport hunting (*23*). We had adequate data for 42 species in the current analysis, including 1 introduced species. Other *Waterbird* species that are not specifically covered by the three plans above are included under the Waterbird Conservation for the Americas initiative (*44*); these include colonial-nesting seabirds, herons, beach-nesting species and secretive marshbirds. *Waterbirds* are most poorly represented in our dataset, as many species are poorly monitored. We had adequate data for 77 species in the current analysis.

We assigned each species to a primary breeding biome and a primary nonbreeding biome, using the Avian Conservation Assessment Database. The ACAD provides broad breeding-habitat categories (e.g., forests, grasslands, oceans) derived from similar categories used to develop habitat indicators for State of the Birds reports in the U.S. and Canada (e.g., (*36*, *45*)), as well as more descriptive sub-categories within major habitats (e.g., Temperate Eastern Forest; Desert Scrub, Freshwater Marsh). All category assignments were based on literature review (primarily BNA accounts) or expert knowledge and underwent extensive review as part of the ACAD process (*66*). Species that use three or more broad habitats in similar importance were considered habitat generalists.

For this paper, we used a combination of *Primary Breeding Habitat* and *Breeding Habitat Description* sub-categories defined in the ACAD to derive a single set of unique breeding biome categories across the North American avifauna (shown in Figure 1A), as follows:

- *Wetlands* = freshwater, inland wetlands; does not include coastal marshes or Arctic tundra.
- *Coasts* = all habitats associated with the Coastal zone, including saltmarsh, beach and tidal estuary, mangroves, and rocky cliffs and islands; includes birds that forage primary in the marine zone
- *Tundra* = Alpine tundra and Arctic tundra, including upland and low, seasonally wet tundra
- *Grasslands* = native grassland, prairie, pasture, and agriculture that supports grassland birds
- *Aridlands* = all arid shrub-dominated communities; primarily in southwestern U.S. and northwestern Mexico; includes ACAD sub-categories of sagebrush, chaparral, desert scrub, barren rocky cliffs, and extensions of tropical dry forest (thornscrub) in southern Texas
- *Boreal forest* = "True" boreal forest of Canada and Alaska; note that some boreal-forest birds also use the boreal zone (primarily spruce-fir) of high mountains in the western and northeastern U.S.
- *Eastern forest* = all temperate forest types of eastern U.S. and southeastern Canada (south of the boreal), including northern hardwoods, oak-hickory, pine-oak, southern pine, and bottomland hardwood associations
- *Western forest* = all temperate forest types of western U.S. and Canada (south of the boreal) and extending in high mountains south into northwestern Mexico; includes Pacific Northwest rainforest, all western conifer, oak-dominated, and riparian forests, pinyon-juniper, juniper-oak woodlands of Edward's Plateau, pine-oak and high-elevation conifer forests of northwestern Mexico
- *Forest generalist* = occurs in similar abundance in two or more forest biomes as described above

- *Habitat Generalist* = occurs in similar abundance in three or more major habitat types, usually including forest and non-forest categories

The ACAD database also lists *Primary Wintering Regions*, in which a majority of the population of each species spends the stationary nonbreeding period during the boreal winter. For this paper we modified and lumped ACAD regions into broader nonbreeding biome categories, using published range maps and eBird distributional data (https://ebird.org/explore), as follows:

- *Temperate North America* = broad region encompassing all of Canada and most of the U.S., excluding arid regions in the Southwest
- *Southwestern Aridlands* = arid regions of southwestern U.S., northwestern Mexico and Mexican Plateau; included species that winter in arid Chihuahuan grassland habitat
- *Mexico-Central America* = combination of ACAD regions within Mexico and Central America, including *Pacific Lowlands, Gulf-Caribbean Lowlands, Mexican Highlands*, and species from *Central and South American Highlands* that winter primarily in Central America
- *South America* = includes *South American Lowlands*, species from *Central and South American Highlands* that winter primarily in South America, and *Southern Cone* ACAD regions
- *Caribbean* = West Indies region, including Cuba, Bahamas, Greater and Lesser Antilles
- *Widespread Neotropical* = occurs in similar numbers in two or more biome regions within the Neotropics
- *Coastal* = coastline habitats throughout the western Hemisphere from Arctic to Atlantic and Pacific Coasts of North, Middle, and South America; eastern Hemisphere coastlines were included to incorporate the main wintering grounds of Pacific Golden-Plover
- *Marine* = littoral zone; area of oceans influenced by continental coastlines; includes bays and deep estuaries (includes a few species that are largely pelagic in the nonbreeding season)
- *Widespread* = occurs in similar abundance in 3 or more nonbreeding biomes, usually encompassing both temperate North American and Neotropical regions
- *Southeast Asia* = overwintering region for Arctic Warbler (and additional Arctic-breeding species not included in the present analysis); note that this nonbreeding biome is not included in summaries presented in Table 1 and Figure S1, but data for Arctic Warbler (Data S1) and included in higher level summaries of population change for all birds, breeding biomes, etc.

<u>Computing vertical profile time series of birds from NEXRAD radar data</u>

While designed to monitor meteorological phenomena (e.g., precipitation, tornados, hail), weather radars routinely detect migrating birds. Weather radar infrastructure represents a biological monitoring tool that achieves an unprecedented spatial and temporal coverage for studying bird migration (*74*). The NEXRAD weather radar network consists of 143 radars in the contiguous US that continuously survey the airspace above the US (*75*). Each of these radars was used to estimate vertical profiles of birds , which summarize a radar's scans completed at a given timestep into the amount, speeds, and directions of birds aloft as a function of altitude. Profile data can be used to accurately estimate migratory biomass abundance and its change throughout the year at comprehensive continental scales (*19*, *77*), an approach we extended here to detect long-

term change in migratory passage across the full US. We restricted our analysis to spring data only (Mar 1 to Jul 1), which is the migratory period closest in time to the breeding bird surveys by BBS. Also, aerial insects are far less numerous in the airspace in early spring as compared to autumn, therefore the spring period allows us to obtain the cleanest bird signal from NEXRAD (see final paragraph of section "Calculating biomass passage from vertical profile time series" below).

Data were obtained from the NOAA-nexrad-level2 public S3 bucket on Amazon Web Services (*78*). Data were analyzed for the period 2007-2018, the period after the Open RDA deployment in NEXRAD (RDA build 7.0), which was a significant upgrade to the Radar Data Acquisition (RDA) functional area of the WSR-88D. In particular, it implemented Gaussian Model Adaptive Processing (GMAP) (*79*, *80*), replacing and improving over the legacy ground clutter filter (*81*) by Doppler filtering. We did not include older potentially lower quality data in the analysis to limit the possibility of legacy filter settings affecting our results. Trend analyses (see following sections for details) controlled for two important data acquisition updates, the gradual upgrades to superresolution (2008-2009) and dual-polarization (2010-2013). The superresolution upgrade increased the azimuthal resolution from 1 to 0.5 degree and range resolution from 1 km to 250 m. The dual-polarization upgrade added functionality to receive horizontally and vertically polarized electromagnetic waves independently, which provided additional products that greatly simplify the classification of meteorological and biological scatterers (*82*).

Night-time polar volumes (level-II data) were processed for all 143 radars in the contiguous US at half-hour interval from 2007-2018 using the vol2bird algorithm (version 0.4.0) (*76*, *83*, *84*), available in R-package bioRad (version 0.4.0) (*83*, *85*). Using cloud computing with 1000 parallel cores on Amazon Web Services (AWS) we reduced this computational task of ~ 4 years on a single CPU to less than a day. Data were processed using the vol2bird algorithm in single-polarization mode (*76*), which requires radial velocity and reflectivity factor information only and no dual-polarization data. Dual-polarization data became available only after mid-2013, and therefore cannot be used for analyses involving older data. In single-polarization mode, resolution samples with high reflectivity values are masked out (η above 36000 cm^2/km^3, i.e., 31 dBZ at S-band / 20 dBZ at C-band, cf. algorithm parameter ETAMAX and paragraph 3.2 in (*76*)), since such high reflectivities are typically associated with precipitation (*76*). The algorithm also identifies contiguous areas of direct neighbors (in a queen's case sense; i.e., diagonal pixels are included as direct neighbors) of reflectivity above 0 dBZ, denoted as reflectivity cells. Cells with a mean reflectivity above 11500 cm^2/km^3 (i.e., 26 dBZ at S-band / 15 dBZ at C-band, cf. algorithm parameter ETACELL and Z_{cell} in (*76*)) are masked from the data. Following recommendations for S-band data discussed in (*83*), we used sd_vvp_threshold=1 m/s (cf. Eq. A2 in (*76*)) and STDEV_CELL=1 m/s (cf. Eq. A3 in (*76*)) to limit masking based on radial velocity texture at S-band.

At S-band, single-polarization mode masks out only the strongest precipitation areas, and weaker precipitation may remain (*83*) (see Figure S3C/E). Precipitation is generally easily identifiable in vertical profiles by experts, based on high reflectivities extending over a relatively large portion of the altitude column (see Figure S3D). Such precipitation cases stand out from bird migration cases, which are characterized by low reflectivities that typically decrease with altitude (see Figure S3A). We used machine learning to develop a full-profile classifier that automatically identifies precipitation-contaminated profiles, as follows.

Years when dual-polarization data were available (2014-2017) were processed a second time in dual-polarization mode (*19*, *83*), which adequately removes precipitation based on high correlation coefficient values (*19*, *82*). These precipitation-free profile data were paired with the single-polarization profile data. By comparing the precipitation-free reflectivity ($\eta_{dualpol}$, cf.

Figure S3A) with the total reflectivity including precipitation (η_{total} derived from reflectivity factor DBZH, cf. Figure S3D), we defined a measure that indicates the range of altitudes H (m) likely containing precipitation, as follows:

$$H = \sum_{i=1}^{n_{\text{layer}}} (\text{if } \eta_{\text{total},i} - \eta_{\text{dualpol},i} > \Delta \text{ then } w_{\text{layer}} \text{ else } 0)$$

with Δ=50 cm^2 km^{-3} (corresponding to 3 dBZ at S-band), and w_{layer} the width of a single altitude layer (200 m). The value of Δ amounts to a fairly low threshold value for classifying potential precipitation, as meteorologists typically assume weak precipitation to start at 7 dBZ (*86*) (133 cm^2 km^{-3} at a 10 cm S-band wavelength), and therefore the vast majority of rain events will show differences in reflectivity exceeding Δ. We labelled all single-polarization profiles in the 4-year dataset with their corresponding H value.

Next, we used gradient boosted trees to detect rain-contaminated profiles computed in single-polarization mode automatically in an unsupervised learning approach, using the H value as our labeling of profiles, with higher H values indicating a wider altitudinal range containing precipitation. We used the R implementation of XGBoost, a highly efficient and scalable gradient boosting algorithm, which can deal with complex nonlinear interactions and collinearity among predictors (*87*, *88*). We used default hyperparameter settings of the xgboost algorithm (learning rate eta=0.3, tree depth max_depth=6, min_child_weight=1, gamma=1, colsample_bytree=1, and subsample=1). Full-profile classifiers were trained for each radar separately. Response variable was the range of altitudes with precipitation H. Predictors included total reflectivity factor (DBZH), precipitation-filtered reflectivity in single-polarization mode (eta), ground speed components (u,v), all at each of the 20 profiles altitude layers, as well as day of year (1-366) and time of day (UTC time). Profiles of each radar were randomly assigned to training (75%) and testing (25%) datasets.

Finally, we determined the parameter H_{max} as the value of H above which profiles are removed in order to discard precipitation contaminations. The value of H_{max} was determined using Figure S4, showing an R-squared measure that quantifies the correspondence between the seasonal migration traffic MT (see next paragraph for definition) of the single-polarization vertical profile time series (with contaminated profiles removed by the full-profile classifier), and the seasonal migration traffic of the reference computed in dual-polarization mode. This R-squared measure amounts to the the coefficient of determination of the scatter points in Figure S5 for a given value of H_{max}. We choose the value of H_{max}=1600 m, producing the best correspondence between the dual-polarization reference and our new single-polarization method. Gaps in a radar's profile time series (after removal of rain-contaminated profiles) of less than 4 hours were filled by linearly interpolating between the neighboring profiles directly before and after the gap.

Applying this value of H_{max} and the full-profile classifier on the testing dataset, we find a precision to correctly classify a profile as rain-contaminated of 99.2%, and a recall of rain-contaminated cases of 97.4%. Precision and recall (*89*) did not depend strongly on the value of the H_{max} threshold, e.g., for H_{max} = 800 m we have a precision of 97.0 % and recall of 99.0%. Our classification performance therefore did not depend critically on the adopted value of the H_{max} parameter.

Calculating biomass passage from vertical profile time series

Nightly reflectivity traffic (RT) (*83*) was calculated for the vertical profile time series of each station for each night with the integrate_profile() function in bioRad (version 0.4.0) (*83*, *85*), which equals the total reflectivity crossing the radar stations per season per one kilometer transect perpendicular to the ground speed direction of movement. Reflectivity traffic is closely related to the amount of biomass that has passed the radar station (*83*). It can be converted to migration traffic (MT), the number of individual birds having passed the radar station per km transect, under assumption of radar cross section (RCS) per individual bird, as in MT = RT/RCS. To express RT in a more intuitive unit, we report MT values in figures using a constant seasonal mean RCS = 11 cm^2 for an individual bird. This value was determined in a calibration experiment spanning a full spring and autumn migration season (*76*), corresponding to passerine-sized birds (10-100 g range) (*90*), which represents the highest-abundance species group dominating our radar signals (*19*). As additional quality control for non-avian signals, we only included altitude layers of profiles for which the ground speed direction was in the northward semicircle surrounding a radar, since migratory bird movements in spring are expected to fall within this semicircle.

Spatial interpolations across the contiguous US of nightly migration traffic were estimated by ordinary kriging with a spherical variogram model, using the R package gstat (*91*). We clipped water areas after interpolating, leaving land areas of the contiguous United States. Missing estimates of nightly migration traffic (e.g., due to temporary radar down time) were imputed from nightly kriging-interpolated maps of MT based on operational stations, imputing the MT value at the location of the inactive radars. Parameters of the spherical variogram model were estimated for each night. In cases where the variogram fit did not converge - typically during nights with very limited migration - we used variogram parameters fit to the average seasonal spring migration traffic (partial sill = 0.577, range = 1093 km). Radar availability was very high, therefore only a small percentage of in total 2.8% of nightly MT values were imputed by this procedure.

Total seasonal migration traffic was calculated as the sum of nightly MT values within a season from Mar 1 to Jul 1. Radar seasons were excluded from trend analysis entirely if data availability dropped below 80% in the period 1 Mar – 1 Jul (4.8% of radar seasons for 143 stations during 11 spring seasons).

While traffic rates suppress any non-migratory stationary signals, like those of non-directed foraging movements of insects or bats (*19*), a small contribution of directed migratory movements of bats or insects could remain in our data. Free-tailed bats in the south are known to show up in radar (*92*) and have a population size estimated up to 100 million individuals (*93*), which amounts to up to a few percent of the total migratory passage of several billion birds along the southern border (*19*). In the North-East - where we observe strongest declines in biomass passage - several migratory tree-dwelling bat species occur, but their population sizes are thought to be smaller than of free-tailed bats. For the period 2013-2017 we have provided earlier a detailed quantitative estimate of the upper limit to the migratory insect contribution to the migratory passage in autumn, when insect abundances are highest. The estimated passage due to insects was 2.1 % (northern US border) – 3.8 % (southern US border) (*19*). Our current study is conducted in spring when aerial insect abundances are far lower (*94*), especially in the North East where we observe most declines, and we estimate the insect contribution to the biomass passage to be on the order of a percent or less.

Calculating trends from seasonal biomass passage values

To correct for potential radar sensitivity changes related to radar processing upgrades, we determined the timing of the upgrade to super-resolution and the upgrade to dual-polarization for

each station. Radar seasons for which the upgrade fell within a migration period were excluded from the analysis. The mode of operation was classified as "legacy" (before superresolution upgrade), "superres" (after superresolution upgrade, before dual-polarization upgrade) or "dualpol" (after dual-polarization upgrade), and stored as a factor variable 'mode' having three factor levels to denote each mode of operation. Variable 'mode' was included in models to correct for changes in operational mode. We also tested for the effect of dual-polarization and superresolution upgrade separately. In these cases, factor variable 'mode' was replaced with a logical explanatory variable 'dualpol' (true after dual-polarization upgrade, otherwise false) or 'superres' (true after superresolution upgrade, otherwise false) in the trend models. The total model candidate set thus contained 4 models, encompassing all combinations of possible corrections for mode of operation, including no correction.

We estimated geographically varying trend patterns using a spatial GAM (*95*) using the mgcv package in R (*39*). Seasonal migration traffic was standardized to each radar's 11-year mean, stored as variable 'index'. We then modeled the spatial trend using an offset tensor product smooth te(lon,lat) and a tensor smooth representing a spatially varying linear trend with year te(lon,lat,by=year) on the linear predictor scale (see Table S3). We used a Gamma distribution with log-link, such that our linear trend smooth term on the linear predictor scale represents a spatially varying annual rate of change μ_{trend} (with standard deviation σ_{trend}) on the response scale. The Gamma distribution accommodates a small right-skew in our continuous positive response variable and warrants normality of deviance residuals, as inspected using QQ plots. Plots of the spatial trend surfaces estimated for the models in Table S3 are shown in Figure S7.

Changes in seasonal migration traffic (Table S4, Figure 2D) were calculated as the GAM prediction for year 2007 minus 2017 (the proportional loss over 11 years), times the 11-year average seasonal migratory traffic (MT) of each station. The surface of average migratory traffic was obtained from a kriging interpolation of the 11-year mean seasonal MT value for each station (see Figure S6, 2). Average trends for the entire US (see main text and Table S3) were averaged over all pixels of these spatially-explicit decline and loss surfaces across the contiguous US, using arithmetic mean and harmonic mean for calculating mean and variance values, respectively, effectively weighing the trend by passage of biomass. The trend value reported in the main text refers to this biomass-weighted average trend for a model average of all GAM models in our candidate set (listed in Table S3). Models were averaged using package MuMIn (*96*), which averages models based on AIC (*97*).

We also estimated continental-wide trends in migratory passage and trends for four flyway regions: Atlantic, Mississippi, Central and Western, following the definitions of the US Fish and Wildlife Service, REF (cf. Figure 2B,C). We fitted generalized linear mixed models using R-package lme4 (*98*), including radar station as a random offset, and region and the interaction year:region as fixed effects, see Table S4 for model structures and Table S5 for estimated model parameters. Like in the GAM analysis, the candidate model set equaled for 4 models, containing all combinations of possible corrections for operational mode.

Regional biomass passage indices (Figure 2A,B) were calculated as the yearly sum of seasonal migration traffic values MT for the radars within each region, standardized by the sum of seasonal migration traffic values MT for all radars in the network of the first year (2007). Values of regionalized decline rates (Atlantic, Mississippi, Central and Western) in the main text are based on the model average (*96*) of all GLMs in the candidate set. Reported errors represent standard errors at a 95% confidence level.

Our GAM analysis (Table S3) and GLM analysis (Table S5) both found support for the dual-polarization upgrade affecting the value of MT, but not for the superresolution upgrade: including variable 'mode' did not produce a more informative model relative to a model with variable 'dualpol' that makes no distinction between "legacy" and "superresolution" data. Effect of the dual-polarization upgrade was a reduction in seasonal migration traffic by a factor 0.85 ± 0.03 (regionalized GLM) or 0.88 ± 0.05 (spatial GAM). Accounting for potential changes in detectability effectively reduced the steepness of decline rates and biomass loss. Both the superresolution and dual-polarization upgrades were designed to prevent changes in detectability and minimize bias effects for meteorological echoes as much as possible, and it is not known whether including correction terms for biological echoes is required. We report versions of the models with and without correction terms such that the effects of these corrections can be compared. By including correction terms, potentially part of the declines in seasonal migration traffic are modelled by the detection-related explanatory variables, and our estimates of decline of models with most information-theoretic support (model 1, model 5) are thus potentially too conservative. Importantly, the presence of an average decline in the passage of migratory biomass is robust to inclusion of correction terms for changes in operational mode of the radar, and even our most conservative rates of decline are alarming.

Supplementary References

33. J. R. Sauer, W. A. Link, J. E. Fallon, K. L. Pardieck, D. J. Ziolkowski, The North American Breeding Bird Survey 1966–2011: Summary Analysis and Species Accounts. *North American Fauna*. 79, 1–32 (2013).

34. K. V. Rosenberg, P. J. Blancher, J. C. Stanton, A. O. Panjabi, Use of North American Breeding Bird Survey data in avian conservation assessments. *The Condor*. 119, 594–606 (2017).

35. J. C. Stanton, P. J. Blancher, K. V. Rosenberg, A. O. Panjabi, W. E. Thogmartin, Estimating uncertainty of North American landbird population sizes. *Avian Conservation and Ecology*. in press (2019).

36. North American Bird Conservation Initiative, The state of Canada's birds, 2012. *Environment Canada, Ottawa, ON* (2012) (available at http://www.stateofcanadasbirds.org/).

37. North American Bird Conservation Initiative, U.S. Committee, "The State of the Birds, United States of America" (U.S. Department of Interior, Washington, DC, 2009).

38. B. Collen, J. Loh, S. Whitmee, L. McRAE, R. Amin, J. E. Baillie, Monitoring change in vertebrate abundance: the Living Planet Index. *Conservation Biology*. 23, 317–327 (2009).

39. S. N. Wood, *Generalized additive models: an introduction with R* (Chapman and Hall/CRC, 2017).

40. W. A. Link, J. R. Sauer, Bayesian Cross-Validation for Model Evaluation and Selection, with Application to the North American Breeding Survey. *Ecology*, 15-1286.1 (2015).

41. K. Rosenberg, J. Kennedy, R. Dettmers, R. Ford, D. Reynolds, J. Alexander, C. Beardmore, P. Blancher, R. Bogart, G. Butcher, Partners in flight landbird conservation plan: 2016 revision for Canada and continental United States. *Partners in Flight Science Committee* (2016).

42. T. Rich, C. Beardmore, H. Berlanga, P. Blancher, M. Bradstreet, G. Butcher, D. Demarest, E. Dunn, W. Hunter, E. Iñigo-Elias, Partners in Flight North American landbird conservation plan. Ithaca, NY: Cornell Lab of Ornithology (2004).

43. S. Brown, C. Hickey, B. Gill, L. Gorman, C. Gratto-Trevor, S. Haig, B. Harrington, C. Hunter, G. Morrison, G. Page, National shorebird conservation assessment: Shorebird conservation status, conservation units, population estimates, population targets, and species prioritization. *Manomet Center for Conservation Sciences, Manomet, MA* (2000).

44. J. A. Kushlan, M. J. Steinkamp, K. C. Parsons, J. Capp, M. A. Cruz, M. Coulter, I. Davidson, L. Dickson, N. Edelson, R. Elliot, Waterbird conservation for the Americas: the North American waterbird conservation plan, version 1 (2002).

45. North American Bird Conservation Initiative, The State of North America's Birds 2016. *Environment and Climate Change Canada: Ottawa, Ontario* (2016) (available at http://www.stateofthebirds.org/2016/).

46. Partners in Flight, Avian Conservation Assessment Database, version 2017. Available at http://pif.birdconservancy.org/ACAD. Accessed on Nov 5 2018.

47. J. R. Sauer, W. A. Link, Analysis of the North American Breeding Bird Survey Using Hierarchical Models. *The Auk*. 128, 87–98 (2011).

48. J. R. Sauer, D. K. Niven, K. L. Pardieck, D. J. Ziolkowski, W. A. Link, Expanding the North American Breeding Bird Survey Analysis to Include Additional Species and Regions. *Journal of Fish and Wildlife Management*. 8, 154–172 (2017).

49. J. R. Sauer, K. L. Pardieck, D. J. Ziolkowski, A. C. Smith, M.-A. R. Hudson, V. Rodriguez, H. Berlanga, D. K. Niven, W. A. Link, The first 50 years of the North American Breeding Bird Survey. *The Condor*. 119, 576–593 (2017).

50. J. A. Veech, K. L. Pardieck, D. J. Ziolkowski, How well do route survey areas represent landscapes at larger spatial extents? An analysis of land cover composition along Breeding Bird Survey routes. *The Condor*. 119, 607–615 (2017).

51. M. F. Delany, R. A. Kiltie, R. S. Butryn, Land cover along breeding bird survey routes in Florida. *Florida Field Naturalist*. 42, 15–28 (2014).

52. J. A. Veech, M. F. Small, J. T. Baccus, Representativeness of land cover composition along routes of the North American Breeding Bird Survey. *The Auk*. 129, 259–267 (2012).

53. C. M. E. Keller, J. T. Scallan, Potential Roadside Biases Due to Habitat Changes along Breeding Bird Survey Routes. *The Condor*. 101, 50–57 (1999).

54. J. B. C. Harris, D. G. Haskell, Land Cover Sampling Biases Associated with Roadside Bird Surveys. *Avian Conservation and Ecology*. 2 (2007), doi:10.5751/ACE-00201-020212.

55. S. L. Van Wilgenburg, E. M. Beck, B. Obermayer, T. Joyce, B. Weddle, Biased representation of disturbance rates in the roadside sampling frame in boreal forests: implications for monitoring design. *Avian Conservation and Ecology*. 10 (2015), doi:10.5751/ACE-00777-100205.

56. M. G. Betts, D. Mitchell, A. W. Diamond, J. Bêty, Uneven Rates of Landscape Change as a Source of Bias in Roadside Wildlife Surveys. *Journal of Wildlife Management*. 71, 2266 (2007).

57. C. U. Soykan, J. Sauer, J. G. Schuetz, G. S. LeBaron, K. Dale, G. M. Langham, Population trends for North American winter birds based on hierarchical models. *Ecosphere*. 7, e01351 (2016).

58. J. Bart, S. Brown, B. Harrington, R. I. Guy Morrison, Survey trends of North American shorebirds: population declines or shifting distributions? *Journal of Avian Biology*. 38, 73–82 (2007).

59. R. K. Ross, P. A. Smith, B. Campbell, C. A. Friis, R. G. Morrison, Population trends of shorebirds in southern Ontario, 1974-2009. *Waterbirds*, 15–24 (2012).

60. M. E. Seamans, R.D. Rau, "American woodcock population status, 2017" (U.S. Fish and Wildlife Service, Laurel, Maryland, 2017), (available at https://www.fws.gov/birds/surveys-and-data/reports-and-publications/population-status.php).

61. U.S. Fish and Wildlife Service, "Waterfowl population status, 2017" (U.S. Department of the Interior, Washington, D.C. USA, 2017), (available at https://www.fws.gov/birds/surveys-and-data/reports-and-publications.php).

62. Anthony D Fox, James O Leafloor, "A global audit of the status and trends of Arctic and Northern Hemisphere goose populations" (Conservation of Arctic Flora and Fauna International Secretariat, Akureyri, Iceland, 2018).

63. D. J. Groves, "The 2015 North American Trumpeter Swan Survey" (U.S. Fish and Wildlife Service, Juneau Alaska, 2017), (available at https://www.fws.gov/birds/surveys-and-data/reports-and-publications.php).

64. K. V. Rosenberg, P. J. Blancher, in *Bird Conservation Implementation and Integration in the Americas: Proceedings of the Third International Partners in Flight Conference 2002 (C.J. Ralph and T.D. Rich, eds.) PSW-GTR-191* (U.S.D.A. Forest Service, Albany, CA, 2005), vol. 191, pp. 57–67.

65. P. Blancher, K. Rosenberg, A. Panjabi, B. Altman, J. Bart, C. Beardmore, G. Butcher, D. Demarest, R. Dettmers, E. Dunn, Guide to the Partners in Flight Population Estimates Database. Version: North American Landbird Conservation Plan 2004. Partners in Flight Technical Series No 5. *US Geological Survey Patuxent Wildlife Research Center, Laurel, Md* (2007) (available at https://www.partnersinflight.org/resources/pif-tech-series/).

66. P. J. Blancher, K. V. Rosenberg, A. O. Panjabi, B. Altman, A. R. Couturier, W. E. Thogmartin, Handbook to the partners in flight population estimates database, version 2.0. *PIF Technical Series* (2013) (available at http://pif.birdconservancy.org/PopEstimates/).

67. W. E. Thogmartin, F. P. Howe, F. C. James, D. H. Johnson, E. T. Reed, J. R. Sauer, F. R. Thompson, A review of the population estimation approach of the North American Landbird Conservation Plan. *The Auk*. 123, 892 (2006).

68. Sea Duck Joint Venture, "Recommendations for Monitoring Distribution, Abundance, and Trends for North American Sea Ducks" (U.S. Fish and Wildlife Service, Anchorage, Alaska and Canadian Wildlife Service, Sackville, New Brunswick, 2007), (available at http://seaduckjv.org).

69. B. A. Andres, P. A. Smith, R. G. Morrison, C. L. Gratto-Trevor, S. C. Brown, C. A. Friis, Population estimates of North American shorebirds, 2012. *Wader Study Group Bull*. 119, 178–194 (2012).

70. U.S. Shorebird Conservation Partnership, "Shorebird Flyway Population Database (Accessed: 28 Feb 2018)" (2016), (available at https://www.shorebirdplan.org/science/assessment-conservation-status-shorebirds/).

71. P. G. Rodewald (Editor), *The Birds of North America* (Cornell Laboratory of Ornithology, Ithaca, NY, USA, 2018; https://birdsna.org).

72. A. O. Panjabi, P. J. Blancher, W. E. Easton, J. C. Stanton, D. W. Demarest, R. Dettmers, K. V. Rosenberg, Partners in Flight Science Committee, "The Partners in Flight handbook on species assessment Version 2017," *Partners in Flight Technical Series No. 3. Bird Conservancy of the Rockies* (Partners in Flight, 2017).

73. Wetlands International, Waterbird Population Estimates (2018), (available at wpe.wetlands.org).

74. S. Bauer, J. W. Chapman, D. R. Reynolds, J. A. Alves, A. M. Dokter, M. M. H. Menz, N. Sapir, M. Ciach, L. B. Pettersson, J. F. Kelly, H. Leijnse, J. Shamoun-Baranes, From Agricultural Benefits to Aviation Safety: Realizing the Potential of Continent-Wide Radar Networks. *BioScience*. 67, 912–918 (2017).

75. T. D. Crum, R. L. Alberty, The WSR-88D and the WSR-88D Operational Support Facility. *Bulletin of the American Meteorological Society*. 74, 1669–1687 (1993).

76. A. M. Dokter, F. Liechti, H. Stark, L. Delobbe, P. Tabary, I. Holleman, Bird migration flight altitudes studied by a network of operational weather radars. *Journal of The Royal Society Interface*. 8, 30–43 (2011).

77. K. G. Horton, B. M. Van Doren, F. A. La Sorte, E. B. Cohen, H. L. Clipp, J. J. Buler, D. Fink, J. F. Kelly, A. Farnsworth, Holding steady: Little change in intensity or timing of bird migration over the Gulf of Mexico. *Global Change Biology* (2019), doi:10.1111/gcb.14540.

78. S. Ansari, S. Del Greco, E. Kearns, O. Brown, S. Wilkins, M. Ramamurthy, J. Weber, R. May, J. Sundwall, J. Layton, A. Gold, A. Pasch, V. Lakshmanan, Unlocking the Potential of NEXRAD Data through NOAA's Big Data Partnership. *Bulletin of the American Meteorological Society*. 99, 189–204 (2018).

79. A. D. Siggia, R. E. Passarelli, in *Proc. ERAD* (2004), vol. 2, pp. 421–424.

80. J. N. Chrisman, C. A. Ray, in *32nd Conference on Radar Meteorology* (2005).

81. R. L. Ice, R. D. Rhoton, D. S. Saxion, C. A. Ray, N. K. Patel, D. A. Warde, A. D. Free, O. E. Boydstun, D. S. Berkowitz, J. N. Chrisman, J. C. Hubbert, C. Kessinger, M. Dixon, S. Torres, in *23rd International Conference on Interactive Information Processing Systems for Meteorology, Oceanography, and Hydrology* (2007).

82. P. M. Stepanian, K. G. Horton, V. M. Melnikov, D. S. Zrnić, S. A. Gauthreaux, Dual-polarization radar products for biological applications. *Ecosphere*. 7, e01539 (2016).

83. A. M. Dokter, P. Desmet, J. H. Spaaks, S. van Hoey, L. Veen, L. Verlinden, C. Nilsson, G. Haase, H. Leijnse, A. Farnsworth, W. Bouten, J. Shamoun-Baranes, bioRad: biological analysis and visualization of weather radar data. *Ecography* (2018), doi:10.1111/ecog.04028.

84. A. M. Dokter, adokter/vol2bird: vol2bird (Version 0.4.0). Zenodo. (2019), (available at http://doi.org/10.5281/zenodo.3369999).

85. A. M. Dokter, S. Van Hoey, P. Desmet, adokter/bioRad: bioRad (Version 0.4.0). Zenodo. (2019), (available at http://doi.org/10.5281/zenodo.3370005).

86. R. J. Doviak, D. S. Zrnić, *Doppler radar and weather observations* (Dover Publications, Mineola, N.Y, 2nd ed., Dover ed., 2006).

87. T. Chen, C. Guestrin, in *Proceedings of the 22nd ACM SIGKDD International Conference on Knowledge Discovery and Data Mining - KDD '16* (ACM Press, San Francisco, California, USA, 2016; http://dl.acm.org/citation.cfm?doid=2939672.2939785), pp. 785–794.

88. T. Chen, T. He, M. Benesty, V. Khotilovich, Y. Tang, *xgboost: Extreme Gradient Boosting* (2017; https://github.com/dmlc/xgboost).

89. J. Davis, M. Goadrich, (ACM, 2006), pp. 233–240.

90. C. R. Vaughn, Birds and insects as radar targets: A review. *Proceedings of the IEEE*. 73, 205–227 (1985).

91. E. J. Pebesma, Multivariable geostatistics in S: the gstat package. *Computers & Geosciences*. 30, 683–691 (2004).

768 92. P. M. Stepanian, C. E. Wainwright, Ongoing changes in migration phenology and winter residency at Bracken
769 Bat Cave. *Global Change Biology*. 24, 3266–3275 (2018).

770 93. A. L. Russell, M. P. Cox, V. A. Brown, G. F. McCracken, Population growth of Mexican free-tailed bats
771 (Tadarida brasiliensis mexicana) predates human agricultural activity. *BMC Evolutionary Biology*. 11 (2011),
772 doi:10.1186/1471-2148-11-88.

773 94. V. A. Drake, D. R. Reynolds, *Radar entomology: observing insect flight and migration* (Cabi, 2012).

774 95. S. N. Wood, Fast stable restricted maximum likelihood and marginal likelihood estimation of semiparametric
775 generalized linear models: Estimation of Semiparametric Generalized Linear Models. *Journal of the Royal*
776 *Statistical Society: Series B (Statistical Methodology)*. 73, 3–36 (2011).

777 96. Kamil Barton, "MuMIn: Multi-Model Inference" (R package version 1.42.1, 2018), (available at
778 https://CRAN.R-project.org/package=MuMIn).

779 97. K. P. Burnham, D. R. Anderson, *Model selection and multimodel inference: a practical information-theoretic*
780 *approach* (Springer, New York, NY, 2. ed., 2010).

781 98. D. Bates, M. Mächler, B. Bolker, S. Walker, Fitting Linear Mixed-Effects Models Using lme4. *Journal of*
782 *Statistical Software*. 67 (2015), doi:10.18637/jss.v067.i01.

783 99. D. W. Winkler, S. M. Billerman, I. J. Lovette, *Bird families of the world: An invitation to the spectacular*
784 *diversity of birds* (Lynx Edicions, 2015).

785 100. R. T. Chesser, K. J. Burns, C. Cicero, J. L. Dunn, A. W. Kratter, I. J. Lovette, P. C. Rasmussen, J. V.
786 Remsen, D. F. Stotz, B. M. Winger, K. Winker, Fifty-ninth Supplement to the American Ornithological
787 Society's Check-list of North American Birds. *The Auk*. 135, 798–813 (2018).

788

789

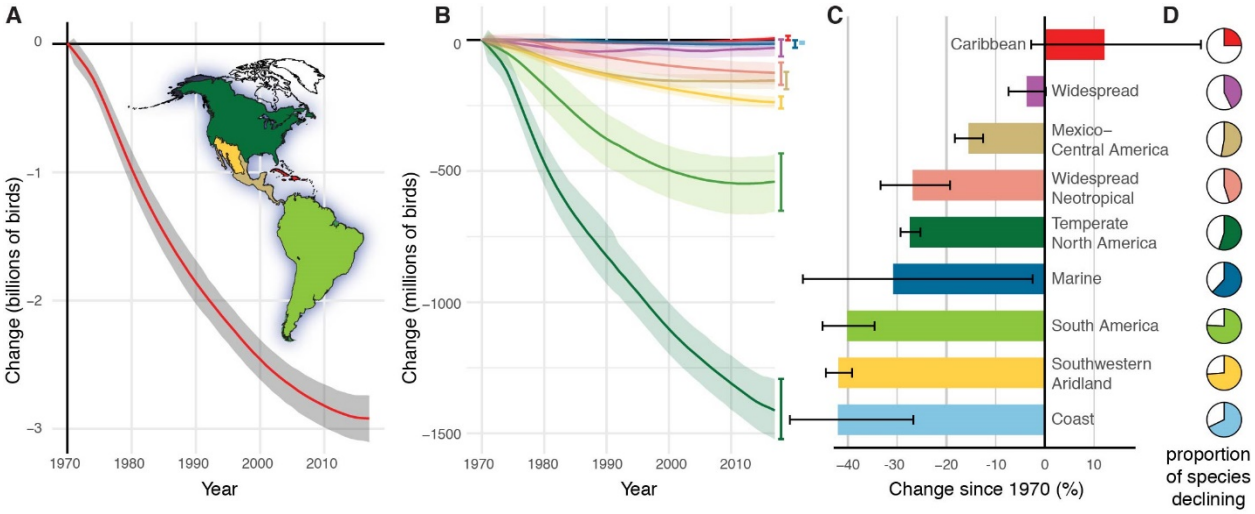

Fig. S1. **Net population change in North American migratory birds grouped by non-breeding biome**. (**A**) By integrating breeding-season population trajectory and size estimates for 529 species (see Methods), we show tthe continental avifauna lost > 2.9 billion breeding birds since 1970. Gray shaded region represents ± 95% credible intervals around total estimated loss. Map shows color-coded non-breeding biomes based on primary overwinter distributions of each species (See Methods). (**B**) Net loss of abundance occurred across all major non-breeding biomes, except Caribbean (see Table 1). (**C**) Proportional population loss, ±95% C.I. (**D**) Proportion of species declining in each biome.

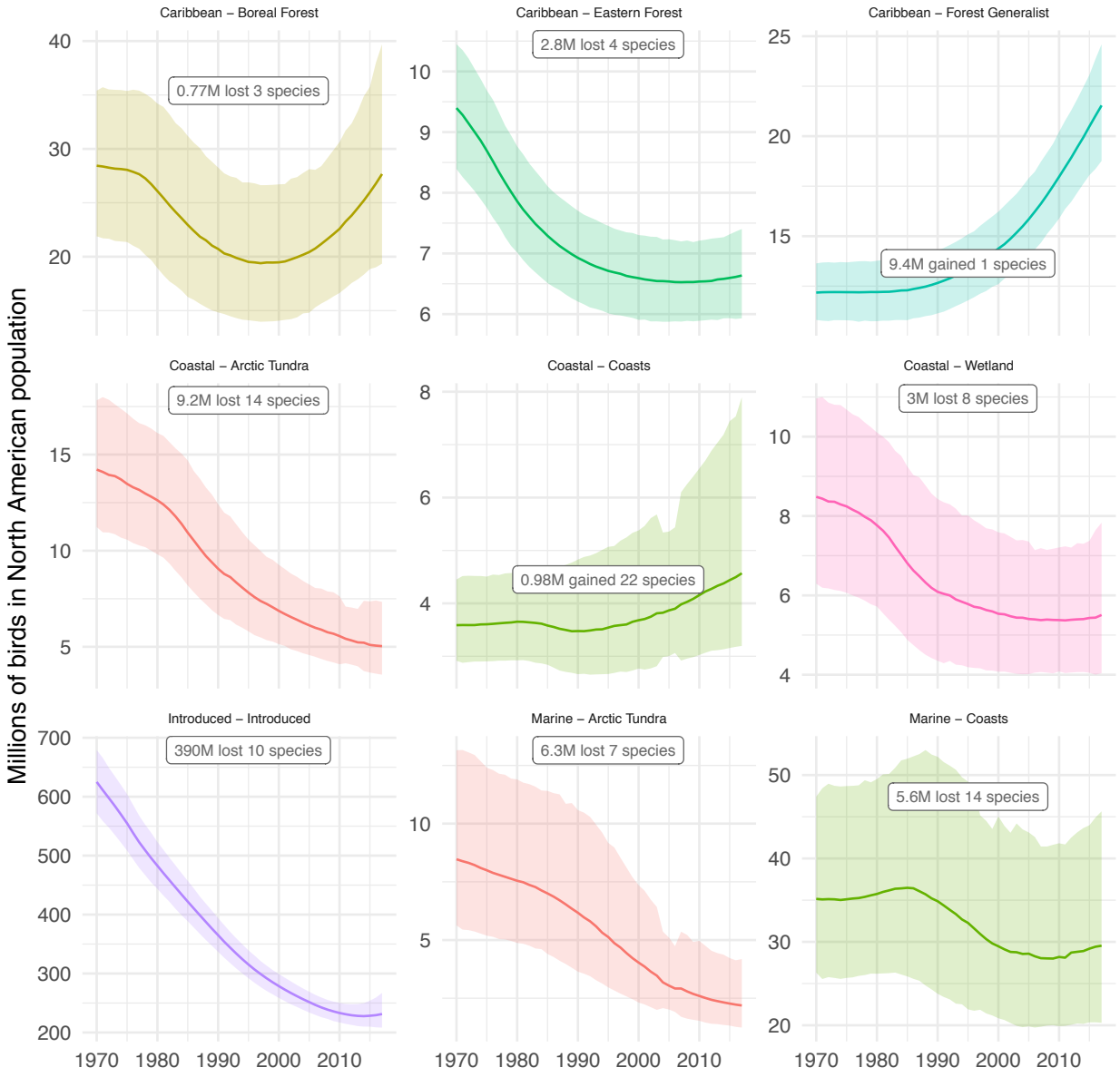
Caribbean – Boreal Forest
0.77M lost 3 species
Caribbean – Eastern Forest
2.8M lost 4 species
Caribbean – Forest Generalist
9.4M gained 1 species
Coastal – Arctic Tundra
9.2M lost 14 species
Coastal – Coasts
0.98M gained 22 species
Coastal – Wetland
3M lost 8 species
Introduced – Introduced
390M lost 10 species
Marine – Arctic Tundra
6.3M lost 7 species
Marine – Coasts
5.6M lost 14 species
Millions of birds in North American population
1970
1980
1990
2000
2010

801

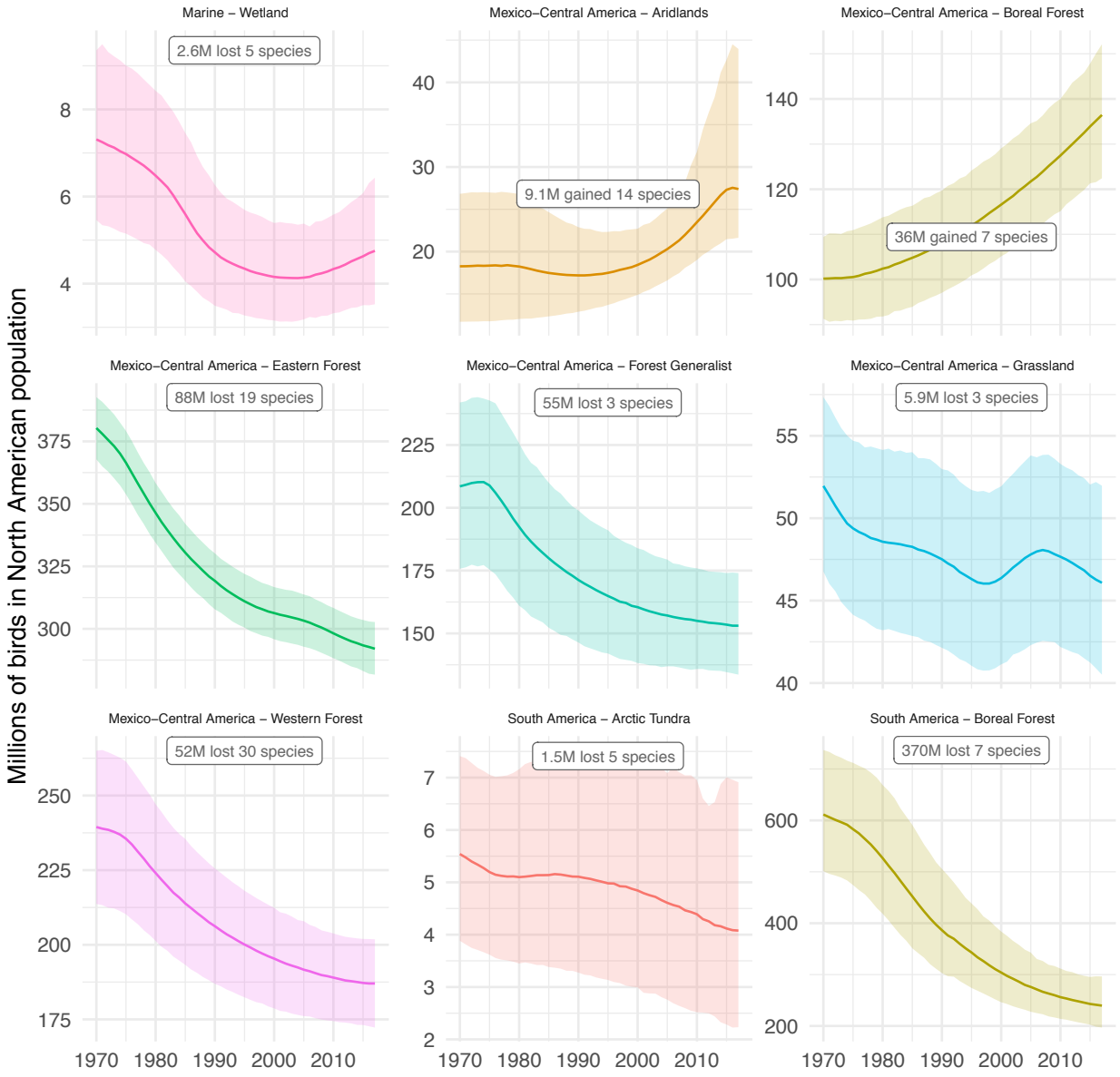
Marine – Wetland
2.6M lost 5 species
Mexico–Central America – Aridlands
9.1M gained 14 species
Mexico–Central America – Boreal Forest
36M gained 7 species
Mexico–Central America – Eastern Forest
88M lost 19 species
Mexico–Central America – Forest Generalist
55M lost 3 species
Mexico–Central America – Grassland
5.9M lost 3 species
Mexico–Central America – Western Forest
52M lost 30 species
South America – Arctic Tundra
1.5M lost 5 species
South America – Boreal Forest
370M lost 7 species
Millions of birds in North American population
1970
1980
1990
2000
2010

802

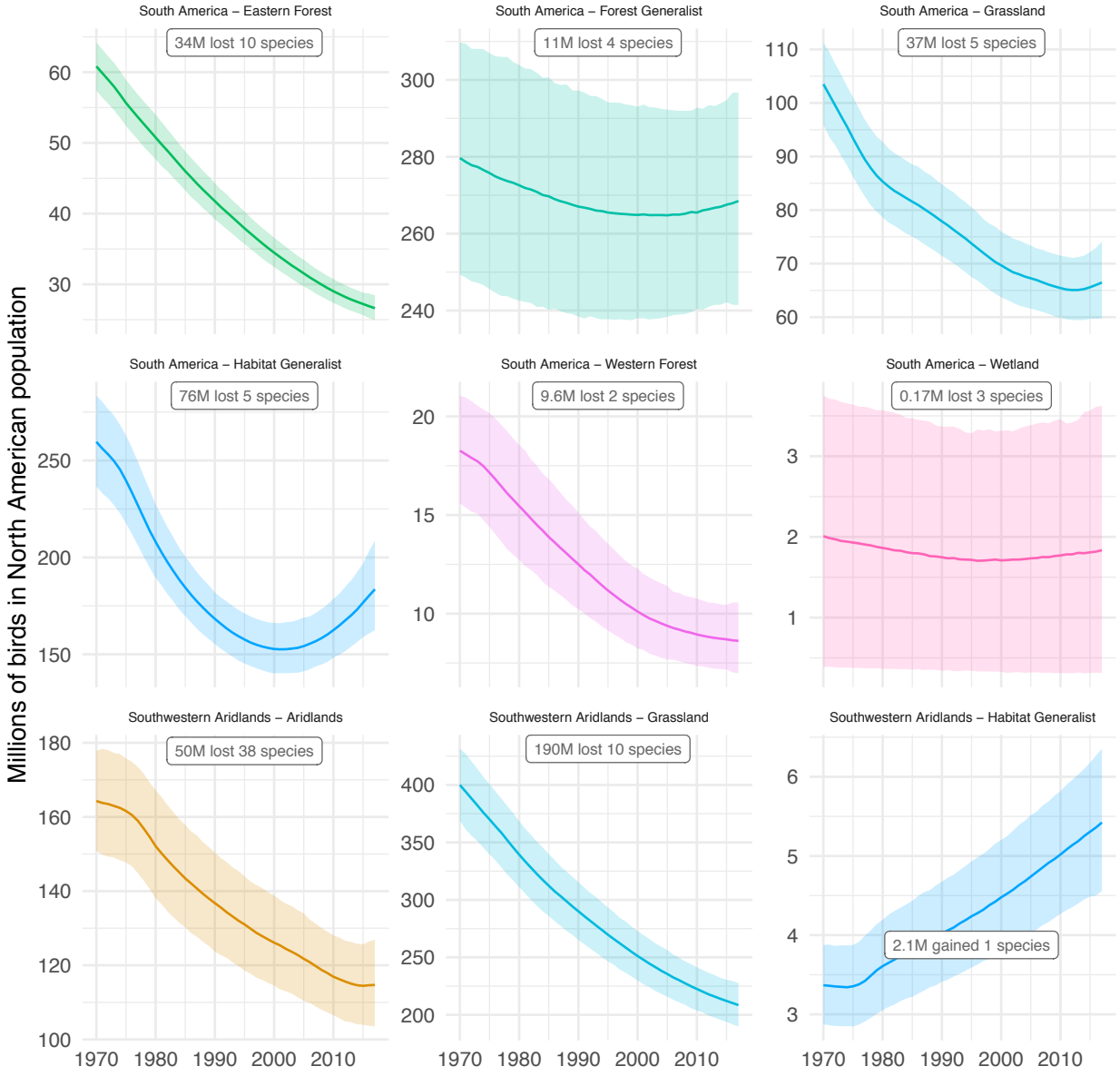
South America – Eastern Forest
34M lost 10 species
South America – Forest Generalist
11M lost 4 species
South America – Grassland
37M lost 5 species
South America – Habitat Generalist
76M lost 5 species
South America – Western Forest
9.6M lost 2 species
South America – Wetland
0.17M lost 3 species
Southwestern Aridlands – Aridlands
50M lost 38 species
Southwestern Aridlands – Grassland
190M lost 10 species
Southwestern Aridlands – Habitat Generalist
2.1M gained 1 species
Millions of birds in North American population
1970
1980
1990
2000
2010

803

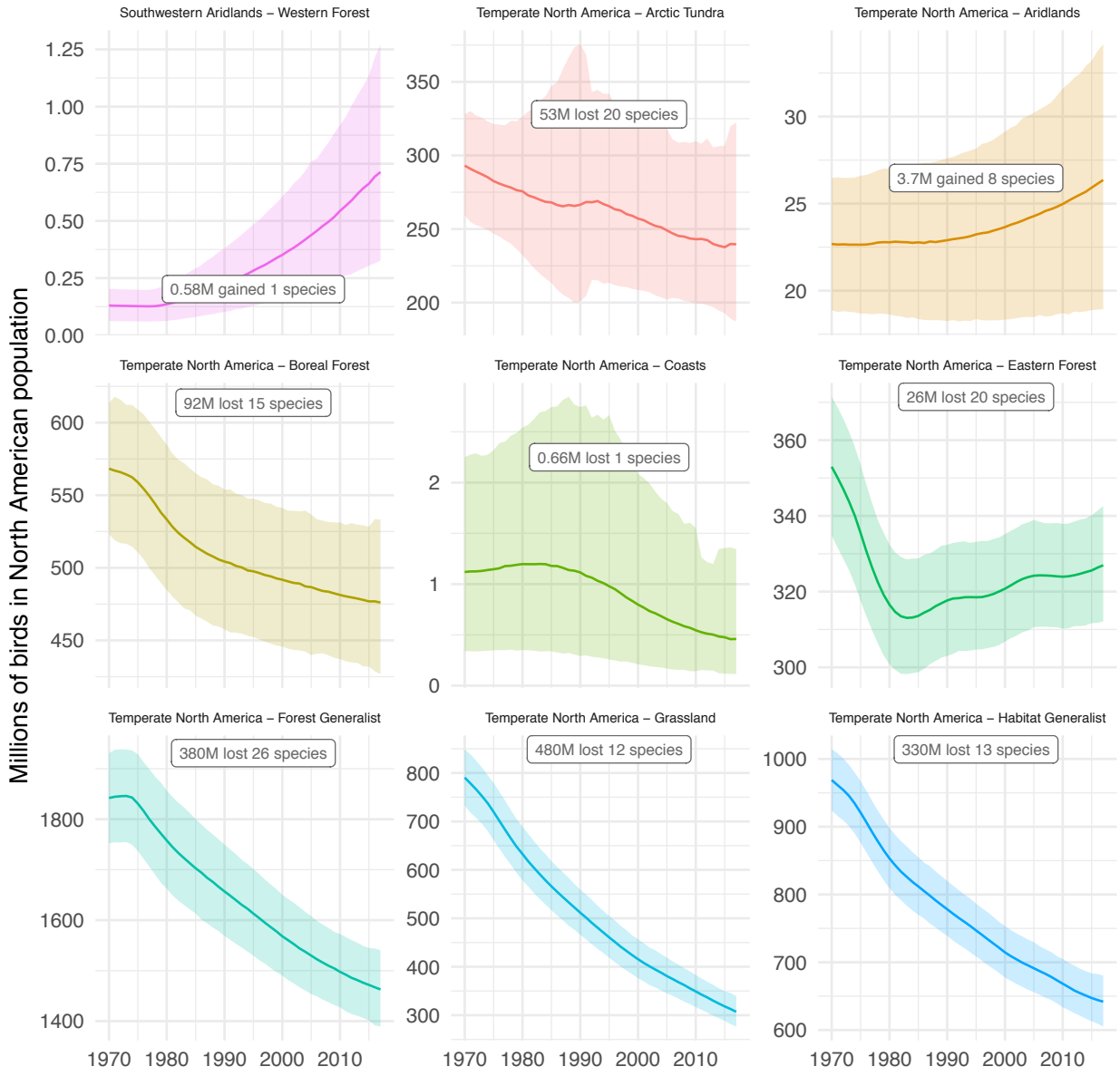
Southwestern Aridlands – Western Forest
0.58M gained 1 species
Temperate North America – Arctic Tundra
53M lost 20 species
Temperate North America – Aridlands
3.7M gained 8 species
Temperate North America – Boreal Forest
92M lost 15 species
Temperate North America – Coasts
0.66M lost 1 species
Temperate North America – Eastern Forest
26M lost 20 species
Temperate North America – Forest Generalist
380M lost 26 species
Temperate North America – Grassland
480M lost 12 species
Temperate North America – Habitat Generalist
330M lost 13 species
Millions of birds in North American population
1970
1980
1990
2000
2010

804

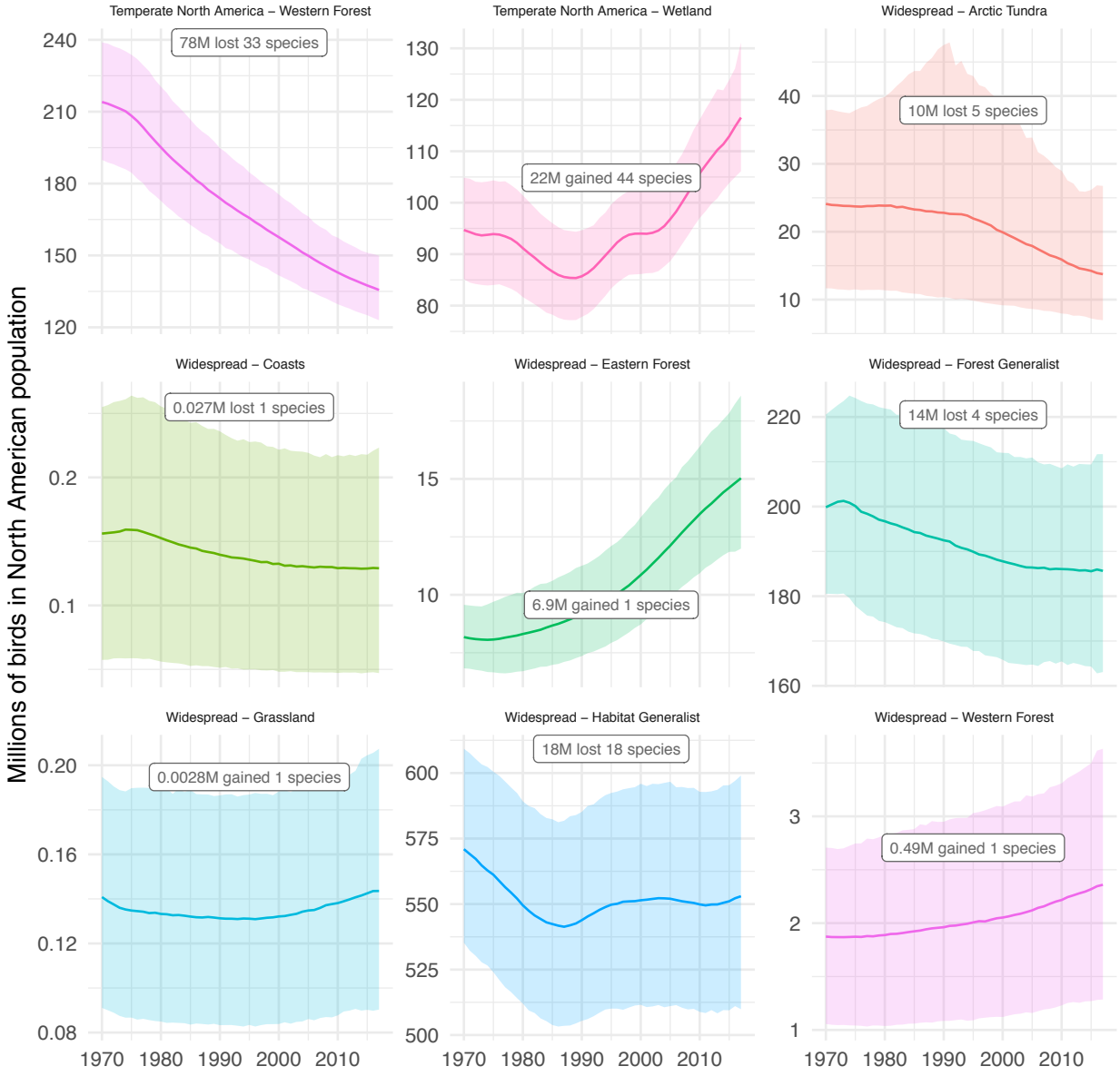
Temperate North America – Western Forest
78M lost 33 species
Temperate North America – Wetland
22M gained 44 species
Widespread – Arctic Tundra
10M lost 5 species
Widespread – Coasts
0.027M lost 1 species
Widespread – Eastern Forest
6.9M gained 1 species
Widespread – Forest Generalist
14M lost 4 species
Widespread – Grassland
0.0028M gained 1 species
Widespread – Habitat Generalist
18M lost 18 species
Widespread – Western Forest
0.49M gained 1 species
Millions of birds in North American population
1970
1980
1990
2000
2010

805

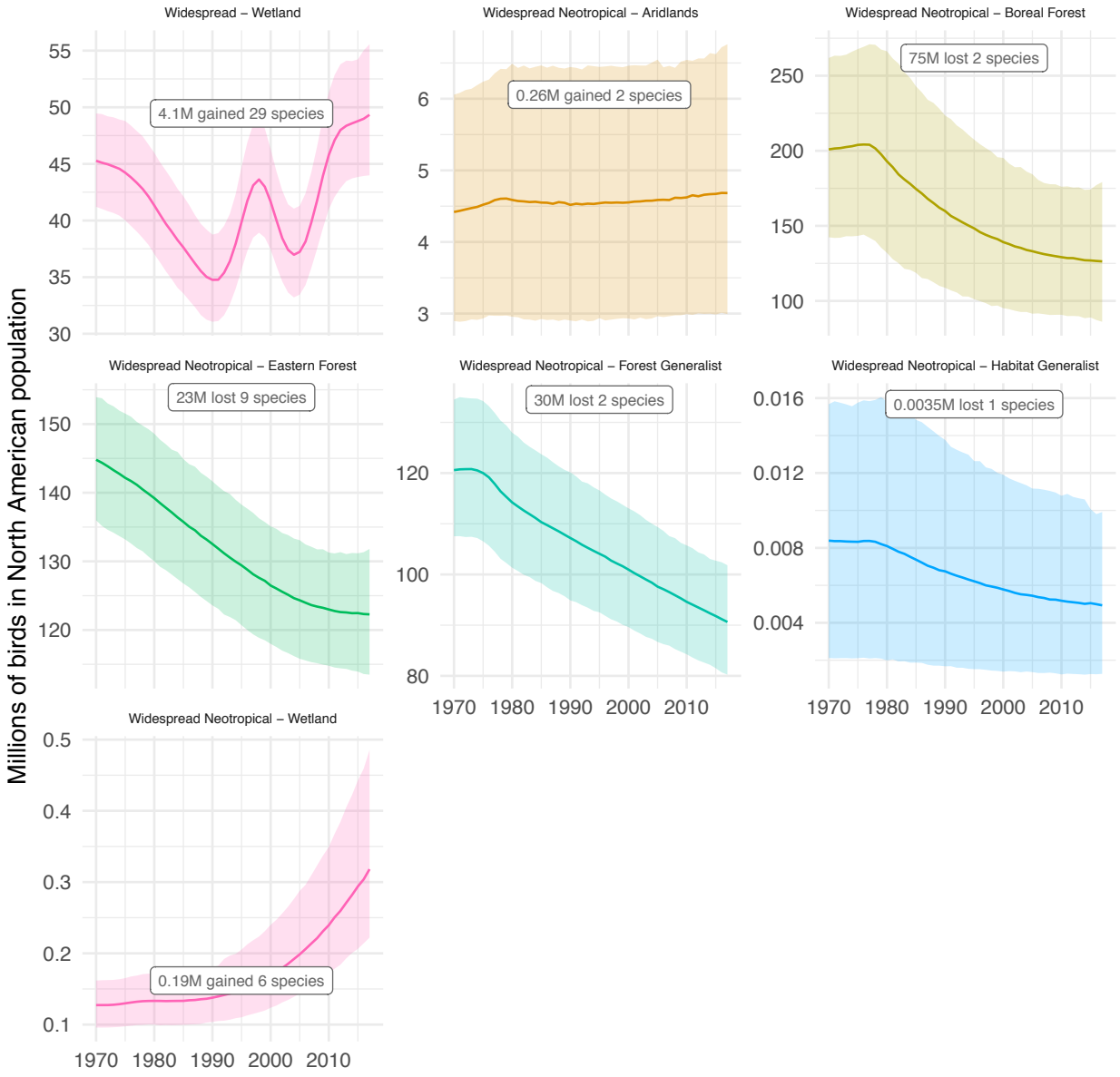

806

807 **Fig. S2.**

808 Change in number of birds in North America by combined nonbreeding and breeding biomes
809 from 1970–2017. Each panel of the figure shows the 1970-2017 trajectory of summed abundance
810 across the species that share a given combination of nonbreeding and breeding biomes (e.g., the
811 first panel shows the trajectory in summed abundance across the 3 species that winter in the
812 Caribbean and breed in the boreal forest). The panel title indicates the wintering biome followed
813 by the breeding biome; labels within the plots show the estimated change in total abundance in
814 millions (M) of birds between 1970 and 2017, and the number of species included in the group.
815 Colored lines and the colored uncertainty bounds represent the median and 95% C.I. of the
816 posterior distribution from the hierarchical Bayesian model. The panels are sorted by
817 nonbreeding biome and the lines are coloured based on the breeding biome.

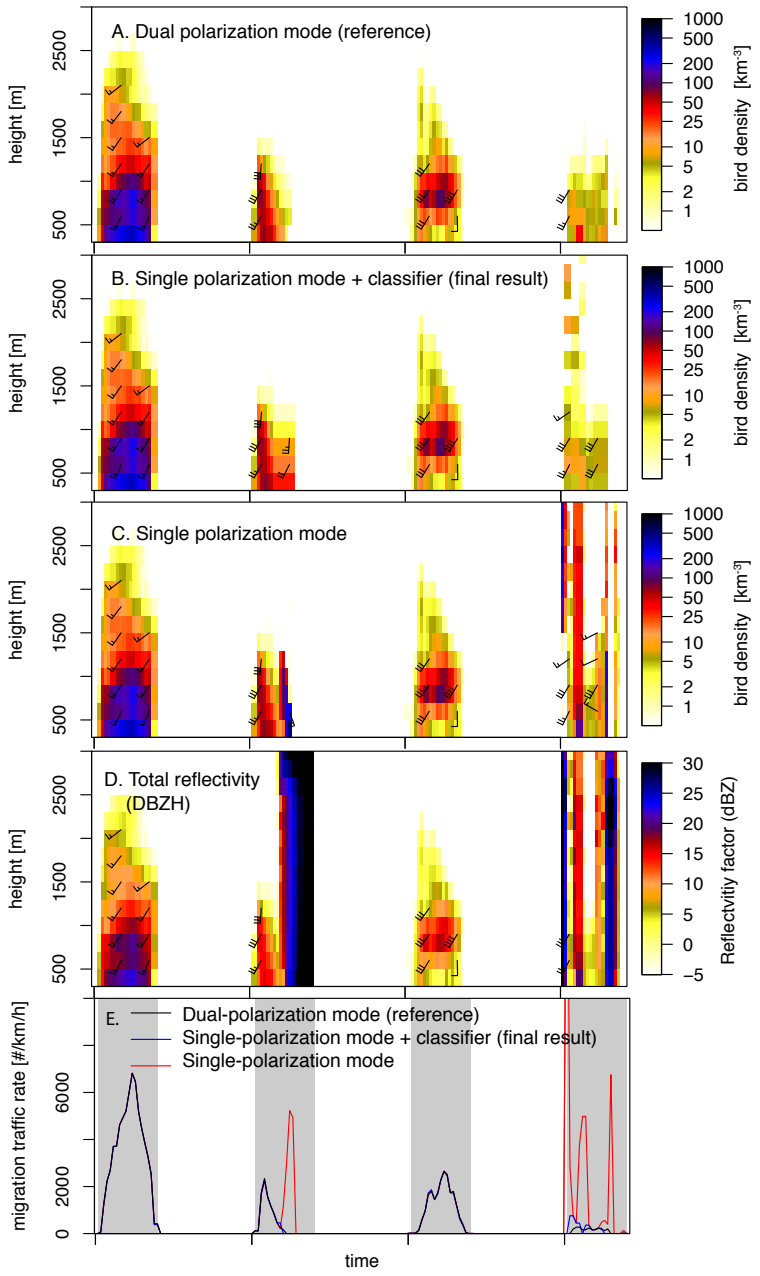

Fig. S3.

Example of vertical profile time series for bird density and speed retrieved in dual polarization mode (A, precipitation-free reference) and the final single-polarization product used in the study (B) for the KBGM radar from 28-31 May 2017. The full-profile classifier that screens precipitation uses the reflectivity product obtained in single-polarization mode (C) and the total reflectivity including precipitation (D). Precipitation is characterized by high reflectivities spanning a large part of the vertical air column (see D), as well by cases in which the single-polarization rain filter removes part (but not necessarily all) of the signal (C versus D). The final single-polarization product (B) closely matches the dual-polarization mode reference (A), see also E, black and blue lines closely overlapping).

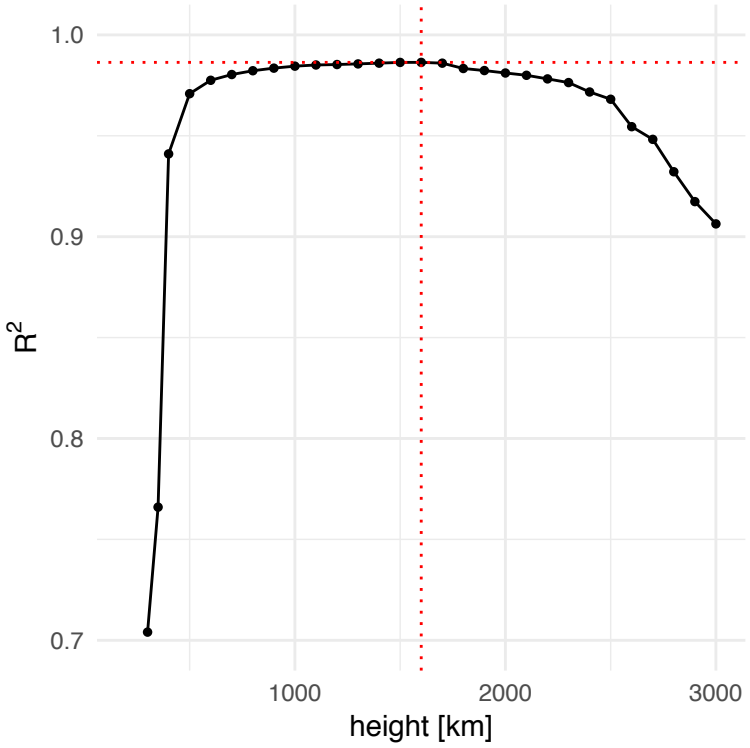

Fig. S4.

Coefficient of determination R^2 between full-spring seasonal migration traffic values calculated in single polarization mode (rain-filtered using full-profile classifier) and dual-polarization mode reference (R^2 based on n=143 stations * 4 years = 572 points), as a function of the classification threshold H_{max}. The value of R^2 peaks at H_{max} = 1600 m .

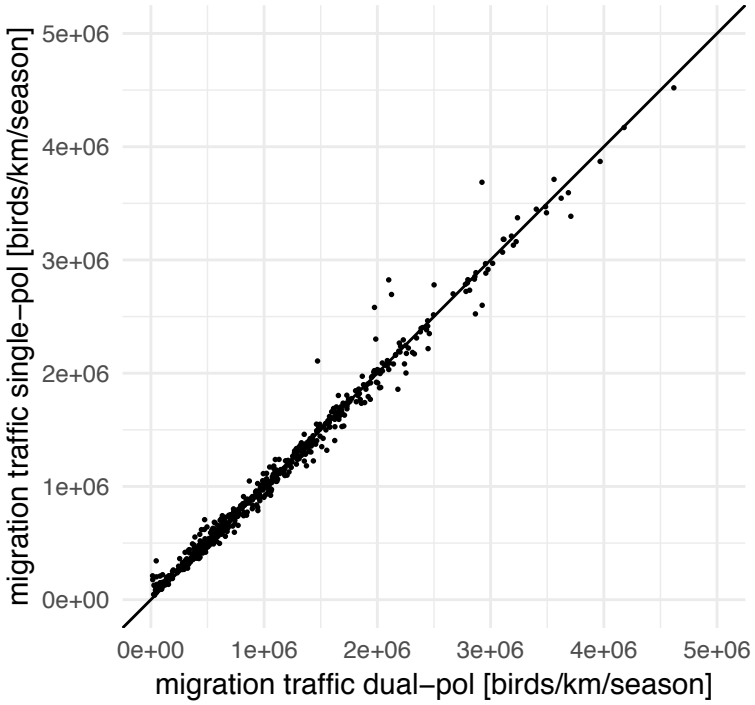

Fig. S5. Seasonal migration traffic (MT) as estimated in dual-polarization mode and in single-polarization mode (rain-filtered using full-profile classifier) for the years 2014-2017 (n=143 stations * 4 year = 572 points). Solid line equals the y=x line of perfect correspondence. This figure shows MT values for H_{max} = 1600 m, which achieves the best correspondence with the dual-polarization reference mode (see Figure S4).

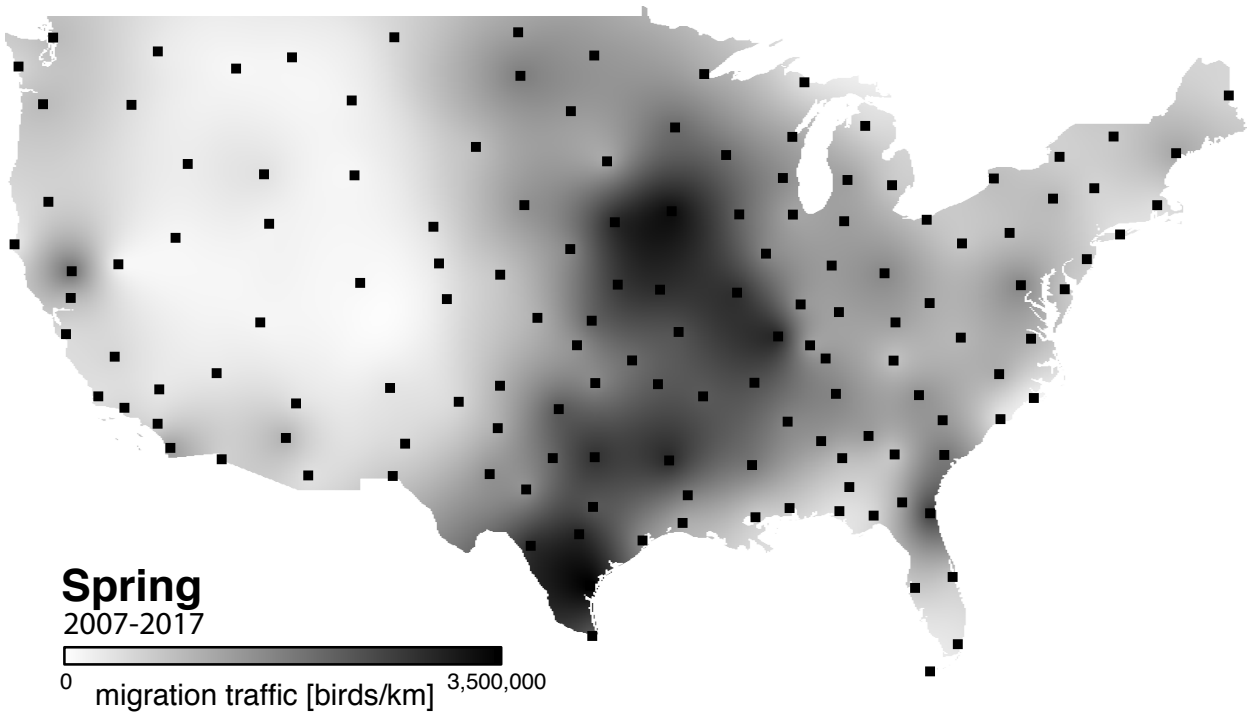

Fig. S6. Cumulated nocturnal migration traffic (biomass passage) MT in spring (1 Mar – 1 Jul) averaged over 11 seasons (2007-2017). Darker colors indicate more migratory biomass passage MT. Values give the numbers of birds passing per 1 km transect perpendicular to the migratory direction per spring season. Radar reflectivity was converted to bird numbers under the assumption of a constant radar cross section of 11 cm^2 per bird. Ordinary kriging was used to interpolate between radar stations. Dots indicate locations of radar station sites.

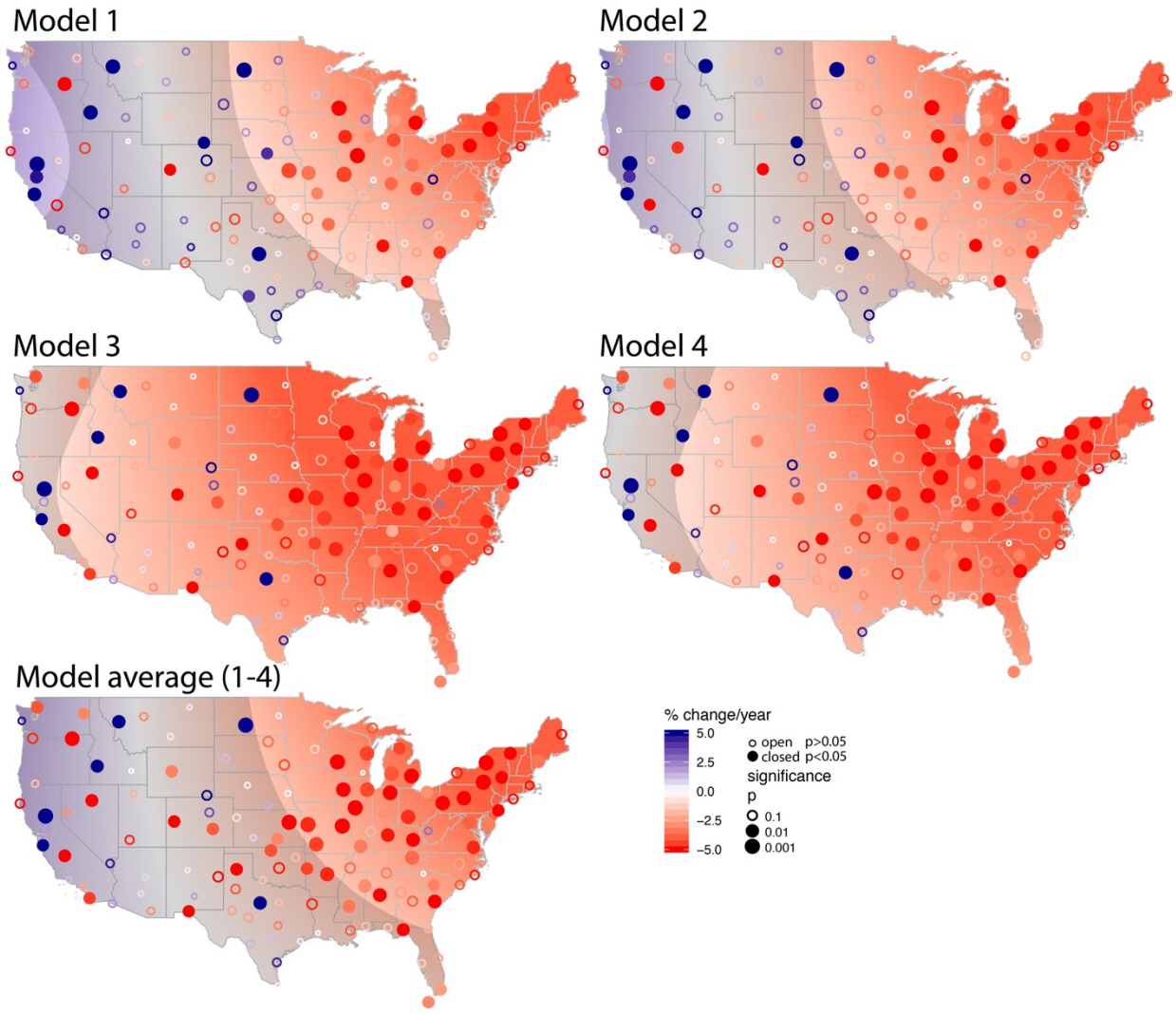

Fig. S7. GAM spatial trend surfaces estimated for the models in Table S3 for the period 2007-2017. Darker red colors indicate higher declines and loss of migration traffic (biomass passage) MT, while blue colors indicate migration traffic increase. Gray shaded regions have an annual rate of change μ_{trend} that is smaller than twice the standard deviation in the rate of change σ_{trend}, i.e. $\mu_{trend} < 2*\sigma_{trend}$. Overlaid circles indicate single-site trend estimates (circle color) and their significance (circle area ~ log(1/p)), with closed circles being significant at a 95% confidence level. Single site trends are fits to seasonal migration traffic data of each radar site separately, using a Generalized Linear Model (GLM) with a Gamma distributional family and log-link. Detectability effects as estimated by the GAM were accounted for in the single-site data prior to fitting the GLMs.

Table S1.

Data sources for population size estimates and population trajectories for 529 North American bird species included in the net population change analysis for the present study. We used published sources of data wherever possible, and applied published methods to calculate estimates for the remaining species. Brief description of methodology, time-span, seasonal, and geographic coverage of surveys and other data sources provided, along with number of species for which that source was used and key citations.

Data source	Years	Season	Methods	Coverage	N Spp. Trajectory	N Spp. Pop	Refs
North American Breeding Bird Survey (BBS)	1970-2017	Breeding	25-mile roadside surveys with 50 3-minute point counts	>4,100 routes in contiguous U.S., southern Canada	415	0	(*33*, *34*, *47*)
North American Breeding Bird Survey (BBS)	1993-2017	Breeding	25-mile roadside surveys with 50 3-minute point counts	Same as above, with additional routes in northern Canada and Alaska	19	0	(*48*)
Audubon Christmas Bird Count (CBC)	1970-2017	Winter	Non-standard counts within 15-mile diameter circles	1,500-2,000 circles in U.S. and Canada	58	0	(*57*)
Partners in Flight (PIF) Population Estimates	2006-2015	Breeding adults	Extrapolation from BBS and other survey count data	Same as BBS, above	0	399*	(*35*)
Arctic goose surveys (CAFF 2018)	1975-2014	Variable	Aerial or ground surveys or mark-recapture models, depending on species	Continentwide for each species	7	7	(*62*)
Shorebird Migration Surveys	1974-2016	Fall migration	Volunteer-conducted surveys at pre-determined sites	Canada and U.S., concentrated in eastern portion	20	0	(*58*, *59*)
USFWS Breeding Waterfowl Surveys	1970-2017	Breeding	Aerial surveys corrected for detectability with ground surveys	2.0 million square miles in Alaska, Canada, and northern U.S.	9	13	(*61*)
North American Trumpteter Swan Survey	1968-2015	Breeding	Aerial surveys and ground counts	Rangewide	1	1	(*63*)
American Woodcock Singing Ground Survey	1968-2017	Breeding	3.6-mile roadside routes	1,500 routes in eastern North America	1	0	(*60*)
2007 Seaduck Joint Venture Report	1970-2007	Variable	Compilation of best available estimates	Continentwide for each species	0	14	(*68*)

Shorebird Flyway Population Database	2012	Breeding population	Compilation of best available estimates	Continentwide for each species	0	45	(*69*, *70*)
Birds of North America (BNA) species accounts	1970-2007	Breeding adults	Variable; best for each species	Continentwide for each species	0	33	(*71*)
Avian Conservation Assessment Database (ACAD)	Variable	Breeding adults	Variable; compiled from other sources	North American estimates	0	17	(*46*)

876 * Estimates for 344 landbird species provided by (*35*); identical methods applied to 55 additional non-landbird
877 species in the present study.
878
879

Table S2.

Net change in abundance across North American bird families, 1970-2017. Taxonomy and common names of families follow (*99*); families listed in order of greatest decline. Net change in abundance expressed in millions of breeding individuals, with upper and lower 90% credible intervals (CI) shown. Percentage of species in each group with negative trend trajectories also noted.

Family	Common Name	N Spp	Net Abundance Change (Millions) & 90% CI			Percent Change & 90% CIs			% Spp in Decline
			Change	UC90	LC90	Change	LC90	UC90	
Passerellidae	New World Sparrows	38	-862.0	-925.7	-798.6	-38.0%	-40.1%	-35.8%	87%
Parulidae	New World Warblers	44	-617.5	-737.8	-509.0	-37.6%	-42.0%	-33.0%	64%
Icteridae	New World Blackbirds	18	-439.8	-467.8	-412.4	-44.2%	-45.9%	-42.4%	83%
Passeridae	Old World Sparrows	2	-331.0	-374.6	-290.2	-81.1%	-82.7%	-79.4%	50%
Alaudidae	Larks	1	-182.0	-207.2	-157.8	-67.4%	-70.9%	-63.7%	100%
Fringillidae	Finches and Allies	13	-144.6	-189.2	-91.9	-36.7%	-45.9%	-23.8%	62%
Tyrannidae	Tyrant Flycatchers	26	-88.2	-107.3	-69.5	-20.1%	-23.7%	-16.2%	50%
Sturnidae	Starlings	1	-83.2	-94.7	-72.6	-49.3%	-52.4%	-46.0%	100%
Turdidae	Thrushes	11	-77.6	-114.2	-38.1	-10.1%	-14.6%	-5.0%	55%
Hirundinidae	Swallows	8	-60.8	-86.7	-31.4	-22.1%	-30.1%	-11.9%	75%
Caprimulgidae	Nightjars	5	-39.3	-44.0	-34.9	-55.0%	-58.0%	-51.5%	60%
Calcariidae	Longspurs	5	-39.3	-79.0	34.3	-31.2%	-60.5%	26.8%	80%
Odontophoridae	New World Quail	5	-21.1	-32.6	-10.0	-51.6%	-61.2%	-35.7%	80%
Laridae	Gulls, Terns	22	-20.1	-27.6	-13.3	-50.5%	-58.4%	-39.9%	73%
Apodidae	Swifts	4	-19.2	-21.4	-17.1	-65.3%	-68.1%	-61.6%	100%
Trochilidae	Hummingbirds	8	-18.9	-36.0	-2.2	-17.0%	-27.7%	-2.6%	63%
Mimidae	Thrashers and Allies	10	-18.3	-22.1	-14.6	-19.4%	-22.9%	-16.0%	80%
Regulidae	Kinglets	2	-17.9	-47.6	12.1	-7.1%	-17.7%	5.0%	50%
Scolopacidae	Sandpipers	32	-15.4	-19.9	-11.1	-38.4%	-46.7%	-28.6%	72%
Cardinalidae	Cardinals and Allies	14	-10.8	-20.6	-1.0	-3.3%	-6.3%	-0.3%	43%
Laniidae	Shrikes	2	-10.3	-11.6	-9.0	-69.0%	-72.2%	-65.7%	100%
Cuculidae	Cuckoos	4	-8.9	-10.5	-7.4	-47.9%	-53.6%	-41.5%	75%
Motacillidae	Pipits, Wagtails	2	-8.1	-12.7	-2.4	-29.0%	-44.0%	-8.6%	100%
Corvidae	Jays, Crows	16	-6.6	-11.8	-1.2	-6.5%	-11.4%	-1.1%	69%
Phylloscopidae	Leaf Warblers	1	-6.4	-16.3	0.7	-50.4%	-76.8%	5.6%	100%
Paridae	Tits, Chickadees	10	-5.3	-11.4	0.8	-4.9%	-10.2%	0.7%	70%
Alcidae	Auks	11	-4.6	-16.8	9.0	-15.9%	-45.8%	33.4%	45%
Icteriidae	Yellow-breasted Chat	1	-3.9	-5.4	-2.5	-21.2%	-28.0%	-13.9%	100%
Ardeidae	Herons	12	-3.4	-4.4	-2.4	-28.0%	-34.1%	-21.2%	58%
Remizidae	Penduline-Tits	1	-2.6	-4.0	-1.4	-42.0%	-53.2%	-28.0%	100%
Charadriidae	Plovers	8	-1.9	-3.1	-0.9	-38.6%	-47.4%	-32.0%	88%

Alcedinidae	Kingfishers	1	-1.6	-1.9	-1.3	-47.8%	-51.5%	-44.0%	100%
Procellariidae	Petrels	1	-1.0	-3.8	3.7	-33.8%	-79.3%	104.4%	100%
Aegithalidae	Long-tailed Tits	1	-0.9	-1.4	-0.3	-28.4%	-42.5%	-10.7%	100%
Podicipedidae	Grebes	6	-0.7	-2.6	1.9	-10.9%	-35.8%	35.7%	50%
Sylviidae	Sylviid Warblers	1	-0.6	-1.1	-0.3	-27.7%	-38.0%	-15.4%	100%
Cinclidae	Dippers	1	-0.03	-0.05	0.00	-15.5%	-27.2%	-2.0%	100%
Aramidae	Limpkin	1	0.00	-0.02	0.02	-15.0%	-62.1%	89.0%	100%
Ciconiidae	Storks	1	0.01	0.00	0.02	77.6%	18.3%	166.9%	0%
Haematopodidae	Oystercatchers	2	0.01	0.01	0.02	123.7%	59.5%	218.0%	0%
Falconidae	Falcons, Caracaras	6	0.03	-0.49	0.63	0.5%	-9.3%	12.6%	33%
Anhingidae	Anhingas	1	0.03	0.02	0.04	109.1%	66.3%	164.5%	0%
Psittacidae	Parrots	1	0.1	0.0	0.3	>1000%	>1000%	>1000%	0%
Tytonidae	Barn Owls	1	0.1	0.1	0.2	211.6%	132.6%	317.8%	0%
Recurvirostridae	Avocets, Stilts	2	0.2	0.0	0.5	57.5%	16.2%	174.6%	0%
Ptiliogonatidae	Silky Flycatchers	1	0.3	0.0	0.7	26.4%	-3.8%	65.2%	0%
Sulidae	Boobies	1	0.4	0.2	0.7	988.6%	497.0%	1891.7%	0%
Gaviidae	Loons	3	0.4	0.1	0.8	32.6%	11.7%	60.7%	33%
Pandionidae	Osprey	1	0.4	0.3	0.5	304.4%	248.4%	370.3%	0%
Rallidae	Rails, Coots	7	0.6	-1.9	4.2	6.2%	-18.1%	40.5%	57%
Gruidae	Cranes	1	0.7	0.5	0.9	914.5%	743.0%	1119.1%	0%
Pelecanidae	Pelicans	2	0.7	0.5	1.2	810.4%	534.6%	1214.2%	0%
Phalacrocoracidae	Cormorants	4	0.8	0.4	1.3	152.3%	73.1%	267.3%	50%
Strigidae	Owls	11	1.7	0.5	3.4	15.9%	4.6%	30.1%	64%
Certhiidae	Treecreepers	1	2.5	1.5	3.7	33.6%	20.8%	47.9%	0%
Threskiornithidae	Ibises, Spoonbills	4	2.9	1.4	6.3	332.8%	167.3%	639.4%	0%
Columbidae	Doves, Pigeons	7	3.6	-17.4	43.3	1.9%	-9.0%	23.1%	57%
Accipitridae	Hawks	16	5.5	5.0	6.0	78.9%	71.8%	86.4%	19%
Bombycillidae	Waxwings	2	8.0	2.1	14.6	13.8%	3.6%	25.0%	50%
Cathartidae	New World Vultures	2	9.4	8.3	10.6	265.3%	238.7%	293.6%	0%
Troglodytidae	Wrens	10	13.3	6.5	20.7	13.8%	6.8%	21.5%	40%
Picidae	Woodpeckers	21	13.6	10.2	17.2	18.5%	13.9%	23.4%	33%
Sittidae	Nuthatches	4	14.4	11.0	18.4	66.6%	50.5%	85.0%	50%
Phasianidae	Grouse and Allies	12	15.2	2.9	36.6	24.3%	4.5%	56.4%	33%
Polioptilidae	Gnatcatchers	2	31.9	12.7	54.5	15.6%	6.2%	26.3%	0%
Anatidae	Waterfowl	42	34.8	24.5	48.3	56.1%	37.9%	79.5%	43%
Vireonidae	Vireos	12	89.9	78.6	102.1	53.6%	46.7%	60.7%	17%

887

Table S3.

GAM spatial trend analysis and model comparison. AIC gives Akaike's An Information Criterion. df gives degrees of freedom. Models significantly different according to a Chi-squared likelihood ratio test are labelled by different letters (a,b). Change in biomass traffic was calculated as a spatial mean of the multiplication of spatial trend and kriging-interpolated biomass passage. Changes in biomass traffic are based on spatial averages of the GAM predictions over the contiguous US, as detailed in the text. From left to right: % / yr = annual rate of decline in seasonal migration traffic, % = decline over the period 2007-2017, loss in seasonal migration traffic, p = significance of the te(lon,lat):year trend term. See Figure S7 for plots of the estimated smoothed spatial trend.

					change in biomass traffic 2007-2017			
Model*	Formula	AIC	df		% / yr	%	10^5 birds/km	p
1	index ~ te(lon,lat) + te(lon,lat):year + dualpol†	337	10	a	-1.2 ± 0.7	-11.6 ± 5.9	-1.4 ± 1.7	<0.0001
2	index ~ te(lon,lat) + te(lon,lat):year + mode‡	338	11	a	-1.6 ± 0.8	-14.8 ± 7.2	-1.8 ± 1.9	<0.0001
3	Index ~ te(lon,lat) + te(lon,lat):year + superres§	342	10	b	-2.9 ± 0.5	-25.6 ± 4.2	-3.2 ± 2.8	<0.0001
4	index ~ te(lon,lat) + te(lon,lat):year	360	9	c	-3.3 ± 0.6	-28.7 ± 4.1	-3.7 ± 3.1	<0.0001
1-4	(model average)				-1.5 ± 1.0	-13.6 ± 9.1	-1.7 ± 1.8	

*Family=Gamma(link=log)

‡mode is a factor variable with levels "legacy", "superres" and "dualpol", distinguishing the three time periods in which the radar acquired legacy, super-resolution and dual-polarization data. Note that the dual-polarization upgrade occurred after the super-resolution upgrade, and dual-polarization data includes super-resolution.

†dualpol is a logical variable that is true after the dual-polarization upgrade, and false before

§superres is a logical variable that is true after the superresolution upgrade, and false before

Table S4.

Model comparison of regionalized generalized mixed models, differentiating in four geographic flyway regions: Atlantic, Mississippi, Central and Western (see Fig. XXX). AIC gives Akaike's An Information Criterion, df degrees of freedom. Models significantly different according to a Chi-squared likelihood ratio test are labelled by different letters (a,b). We found support for an effect of dual-polarization upgrade on detected biomass passage (cf. model 5), but not for additional correction for the superresolution upgrade (model 6 did not improve over model 5). See Table S5 for fixed effect estimates.

Model*	Formula	AIC	df	
5	index ~ region + year:flyway + (1 | radar) + dualpol†	338	11	a
6	index ~ region + year:flyway + (1 | radar) + mode‡	340	12	a
7	Index ~ region + year:flyway + (1 | radar) + superres	343	11	b
8	Index ~ region + year:flyway + (1 | radar)	361	10	c

*Family=Gamma(link=log)

‡mode is a factor variable with levels "legacy", "superres" and "dualpol", distinguishing the three time periods in which the radar acquired legacy, super-resolution and dual-polarization data. Note that the dual-polarization upgrade occurred after the super-resolution upgrade, and dual-polarization data includes super-resolution.

†dualpol is a logical variable that is true after the dual-polarization upgrade, and false before

§superres is a logical variable that is true after the superresolution upgrade, and false before

Table S5.

Parameter estimates of temporal and detection-related fixed effects, based on generalized mixed models differentiating in three geographic regions: west (lon < -105°), central (-105° < lon < -95°) and east (lon> -95°). Estimates of change in migratory biomass traffic are expressed as percentages change per year. Explanatory variable year was scaled to zero at 2007. Significant model terms are highlighted in **bold**. See Table S4 for model comparisons.

Model	Fixed effect	Estimate	Unit	t	p
5	**year:flyway_Atlantic**	**-3.0 ± 0.6**	**%/yr**	**-4.7**	**<0.0001**
5	**year:flyway_Mississippi**	**-2.7 ± 0.6**	**%/yr**	**-4.5**	**<0.0001**
5	year:flyway_Central	0.6 ± 0.6	%/yr	1.0	0.3
5	year:flyway_Pacific	0.2 ± 0.6	%/yr	0.3	0.8
5	**dualpol=TRUE**	**-16 ± 3**	**%**	**-5.0**	**<0.0001**
6	**year:flyway_Atlantic**	**-3.4 ± 0.7**	**%/yr**	**-4.5**	**<0.0001**
6	**year:flyway_Mississippi**	**-3.0 ± 0.7**	**%/yr**	**-4.2**	**<0.0001**
6	year:flyway_Central	0.2 ± 0.7	%/yr	0.3	0.7
6	year:flyway_Pacific	0.1 ± 0.8	%/yr	-0.2	0.9
6	mode="superres"	25 ± 27	%	0.9	0.4
6	**mode="dualpol"**	**-12 ± 5**	**%**	**-2.4**	**0.02**
7	**year:flyway_Atlantic**	**-4.7 ± 0.5**	**%/yr**	**-9.9**	**<0.0001**
7	**year:flyway_Mississippi**	**-4.4 ± 0.4**	**%/yr**	**-10.2**	**<0.0001**
7	**year:flyway_Central**	**-1.2 ± 0.4**	**%/yr**	**-2.7**	**0.007**
7	**year:flyway_Pacific**	**-1.5 ± 0.5**	**%/yr**	**-3.0**	**0.003**
7	**superres=TRUE**	**8 ± 2**	**%**	**4.4**	**<0.0001**
8	**year:flyway_Atlantic**	**-5.2 ± 0.5**	**%/yr**	**-10.9**	**<0.0001**
8	**year:flyway_Mississippi**	**-4.8 ± 0.4**	**%/yr**	**-11.3**	**<0.0001**
8	**year:flyway_Central**	**-1.5 ± 0.4**	**%/yr**	**-3.5**	**0.0004**
8	**year:flyway_Pacific**	**-1.9 ± 0.5**	**%/yr**	**-3.8**	**0.0001**
5-8 (average)[†]	**year:flyway_Atlantic**	**-3.2 ± 0.8**	**%/yr**	**4.1**[*]	**<0.0001**
5-8 (average)[†]	**year:flyway_Mississippi**	**-2.9 ± 0.7**	**%/yr**	**3.9**[*]	**0.0001**
5-8 (average)[†]	year:flyway_Central	0.4 ± 0.8	%/yr	0.5[*]	0.6
5-8 (average)[†]	year:flyway_Pacific	0.3 ± 0.8	%/yr	0.0[*]	1.0

[*]z value instead of t value

[†]showing full model-averaged coefficients for temporal fixed effects only

936

937 **Data S1. (separate file)**

938 **Species-specific data and results for analysis of net population change in the North American**
939 **avifauna**. Included are 529 species with common and scientific names, taxonomic sort number
940 (*100*), bird family, species group and biome assignments, absolute and proportional changes in
941 abundance with associated variance, start and end-year population estimates with variance, and
942 source data for population size estimates and population trajectories for each species. A separate
943 worksheet in the same file contains definitions of each column header.
944

945 **Data S2. (separate file)**

946 **Species-specific adjustment factors used in the calculation of Partners in Flight (PIF)**
947 **population size estimates based on BBS count data**. Included are 399 species, including 344
948 landbird species previously published in (*35*), and 55 additional non-landbird species for which
949 we estimated population size using identical methods. Unrounded population size estimates
950 (PopUsCa) ate the same as in Data S1, and are provided here for easy reference. Adjustment factors
951 are further defined and described in (*35*).
952
953
954